The need for high-quality oocyte mitochondria at extreme ploidy dictates mammalian germline development

Authors: Marco Colnaghi[1,2], Andrew Pomiankowski[1,2*] & Nick Lane[1,2*]

ORCID

0000-0002-5641-9324 (MC)

0000-0002-5171-8755 (AP)

0000-0002-5433-3973 (NL)

Affiliations:

[1]CoMPLEX and [2]Department of Genetics, Evolution and Environment

University College London

Darwin Building, Gower Street, London WC1E 6BT

* **Corresponding author**: Andrew Pomiankowski (ucbhpom@ucl.ac.uk)

One sentence summary (30 words max):

Selective transfer of mitochondria in the Balbiani body ensures high-quality oocyte mitochondria at extreme ploidy, explaining many enigmatic features of female germline architecture including germ cell loss.

ABSTRACT

Selection against deleterious mitochondrial mutations is facilitated by germline processes, lowering the risk of genetic diseases. How selection works is disputed: experimental data are conflicting and previous modelling work has not clarified the issues. Here we develop computational and evolutionary models that compare the outcome of selection at the level of individuals, cells and mitochondria. Using realistic *de novo* mutation rates and germline development parameters from mouse and humans, the evolutionary model predicts the observed prevalence of mitochondrial mutations and diseases in human populations. We show the importance of organelle-level selection, seen in the selective pooling of mitochondria into the Balbiani body, in achieving high-quality mitochondria at extreme ploidy in mature oocytes. Alternative mechanisms debated in the literature, bottlenecks and follicular atresia, are unlikely to account for the clinical data, because neither process effectively eliminates mitochondrial mutations under realistic conditions. Our findings explain the major features of female germline architecture, notably the longstanding paradox of over-proliferation of primordial germ cells followed by massive loss. The near-universality of these processes across animal taxa makes sense in light of the need to maintain mitochondrial quality at extreme ploidy in mature oocytes, in the absence of sex and recombination.

Keywords: Balbiani body, bottleneck, germline, mitochondria, mitochondrial mutation, mtDNA, oogenesis

INTRODUCTION

In mammals, mitochondrial gene sequences diverge at 10-30 times the mean rate of nuclear genes [1, 2]. This difference is typically ascribed to a faster underlying mutation rate and limited scope for purifying selection on mitochondrial genes, given uniparental inheritance, negligible recombination and high ploidy [3]. At face value, weak selection against mitochondrial mutations might seem to be consistent with the high prevalence of mitochondrial mutations (~1 in 200) [4] and diseases (~1 in 5000 births) [5] in human populations. But it is not consistent with the strong signal of purifying selection [6], evidence of adaptive change [7] and codon bias [8] in mitochondrial genes, nor with the low transmission rate of severe mitochondrial mutations between generations [9-11]. Despite the high rate of sequence divergence, female germline processes apparently facilitate selection against mitochondrial mutations, but the mechanisms are disputed and poorly understood [12].

Here we develop computational and evolutionary models that compare three hypotheses of germline mitochondrial inheritance and selection: (i) selection at the individual level, facilitated by mitochondrial bottlenecks; (ii) selection at the cell level through follicular atresia, which weeds out primordial germ cells with high mutation load; and (iii) selection at the organelle level through selective transfer of mitochondria into oogonia during development. These modes of selection are not mutually exclusive nor the only ones that operate (a full examination is provided in the Discussion). The objective here is to clearly delineate the major forces involved and the effectiveness of each in controlling mutation accumulation. Our approach incorporates important factors neglected in earlier work, in

70 particular the input of *de novo* mitochondrial mutations and their segregation over multiple
71 rounds of germ-cell division. This provides a realistic model of mutation, segregation and
72 selection allowing the three hypotheses to be tested against the observed levels of
73 mitochondrial mutation and fitness across a variety of species with an emphasis on the
74 detailed clinical reports in human populations [4, 5].
75
76 The idea that mitochondrial mutations are winnowed through a tight germline bottleneck is
77 pervasive in the literature and has long been held to explain sharp changes in mutation load
78 between generations [13-15]. The exact size of the bottleneck is unclear, with estimates
79 from mouse [16-18] and human studies [14, 19-21] spanning two orders of magnitude.
80 Bottlenecks generate variance in mutation loads among the resulting germ cells, and tighter
81 bottlenecks produce greater variance, offering scope for selection against mitochondrial
82 mutations at the level of the individual [22-24]. The problem with this line of thinking is that
83 it ignores two other forces. First, gametes are produced through multiple rounds of cell
84 division, leading to repeated rounds of mitochondrial segregation, which in itself generates
85 considerable variance [25]. Second, bottlenecks induce greater input of *de novo* mutations
86 as more rounds of mitochondrial replication are required to regenerate the extreme ploidy
87 of mitochondrial DNA in mature oocytes. By applying realistic segregation dynamics and
88 mutational input, we evaluate the impact of these forces on the value of bottleneck size on
89 individual fitness.
90
91 Follicular atresia is another force widely considered to be critical in maintaining oocyte
92 quality [26-28] . In humans [29, 30], the number of germ cells declines dramatically in the
93 foetus between mid-gestation (~20 weeks in humans) when there are 7-8 million oocytes,

to late gestation when at least two thirds of these are lost, leaving a reserve of 1-2 million at birth [31]. Oocyte loss continues throughout the life of an individual, eventually leading to the depletion of the ovarian pool and loss of reproductive function at menopause [32-34]. Similar loss of female germ cells before sexual maturity is evident in mice and several other animal species [35-38]. This attrition has historically been ascribed to cell death during oocyte maturation [39, 40], but more recent findings implicate the apoptotic loss of 'nurse cells' during the genesis of primary oocytes [41]. In either case, differential oocyte loss offers scope for between-cell selection. However, the basis for between-cell selection has long been questioned, on the grounds that it seems unlikely that 70–80% of oocytes have low fitness as a result of mitochondrial mutations [40]. We therefore test whether selection against oocytes with higher loads of mitochondrial mutations during follicular atresia is capable of giving rise to the distribution of mutations observed.

A more recent interpretation of germ-cell loss links it to the formation of the Balbiani body, a prominent feature of the humans [42, 43] and mouse [41, 44-46] female germline, as well as a range of other vertebrates and invertebrates, with a range of terminology (e.g. fusome, mitochondrial cloud) [41, 44-48]. In the mouse, proliferating germ cells typically form clusters of 5-8 cells that establish cytoplasmic bridges [41, 49]. It is thought that around half the mitochondria from each nurse cell are streamed into the Balbiani body of the primary oocyte, through an active cytoskeletal process that depends in part on the membrane potential of discrete mitochondria [50, 51]. This offers scope for purifying selection through the preferential exclusion of dysfunctional mitochondria. The remaining nurse cells, now denuded of half their mitochondria, undergo apoptosis [41]. Selective transfer and pooling of mitochondria from interconnected cells may occur in other vertebrate and invertebrate

systems. We consider the consequence of different strengths of selection at the level of mitochondrial function in the production of the Balbiani body.

To systematically distinguish between the predictions of these three different hypotheses, under a range of reasonable parameter values, we use a computational model to evaluate the patterns of mutation load generated over a single generation in each case. We then use an evolutionary model to generate equilibrium levels and compare the predictions to the prevalence of mutations and disease from human studies. Our results show that selection at the organelle level through the pooling of high-quality mitochondria into the Balbiani body is a more potent force than germline bottlenecks and follicular atresia and must play a key role in the maintenance of mitochondrial function in the face of pervasive mutational pressure. This analysis also pleasingly clarifies the longstanding paradox of germ-cell over-proliferation followed by massive loss which is a widely conserved feature of the female germline in animal taxa.

RESULTS

Computational model

The computational model follows the distribution of mitochondrial mutations across a single generation, using model parameters derived from human data [29] (**Figure 1**). The zygote is assumed to have around half a million copies of mitochondrial DNA (exact number 2^{19}), which are randomly partitioned to the daughter cells at each cell division. The pattern of segregation is in agreement with recent evidence for actin-mediated mixing of mitochondria within cells during mitosis leading to random segregation [52]. We assume independent segregation of mitochondria with one mtDNA per mitochondrion, and do not

consider complications that might arise from the packaging of multiple mtDNA copies per mitochondrion [14]. This assumption is supported by evidence that mitochondrial networks fragment into multiple smaller structures at cell division [53, 54] that probably contain one or a few mtDNAs.

Mitochondrial replication is not active during early embryo development [55], so the mean mitochondrial number per cell approximately halves with each division (**Figure 1B**). In humans, after 12 cell divisions a random group of 32 cells form the primordial germ cells (PGC) [56], which in the model corresponds to a mean of 128 mitochondria per PGC. Mitochondrial replication resumes at this point [29, 55]. Each mtDNA doubles prior to cell division. With probability μ, one of the daughter mitochondria acquires a new deleterious mutation through a copying error. We consider μ in the range 10^{-9} to 10^{-8} to 10^{-7} per base pair per cell division (designated low, standard and high respectively), consistent with the range of estimates for the female germline, and assume no back mutations (see Methods). Point mutations during replication are the dominant form of mutation in mtDNA, so we do not consider damage from other sources such as oxidative damage [57]. Mitotic proliferation of PGCs gives rise to ~8 million oogonia, which are reduced to ~1 million primary oocytes during late gestation (**Figure 1B**) [29, 55]. Proliferation is followed by a quiescent phase during which the mitochondria in primary oocytes are not actively replicated. Mutations accumulate far more slowly during this phase, which persists over decades in humans [55, 58]. For simplicity, we assume no mutational input during this period (not marked in **Figure 1B**). At puberty, the primary oocytes mature through clonal amplification of mitochondria back to the extreme ploidy in mature oocytes (~500,000

165 copies; **Figure 1B**) [59]. The same copying error mutation rate μ is applied during this
166 process.
167
168 We consider three different forms of selection on mitochondria: selection at the level of
169 individuals, cells, or mitochondria. We apply selection at the level of individuals on the
170 zygotic mutation load. Selection at the level of cells or mitochondria is applied during culling
171 at late gestation when primary oocytes are produced. Each of these processes can be
172 captured by modifications of the computational model, allowing easy comparison between
173 them. In order to distinguish between different levels of selection, the model extends earlier
174 work that considered segregational variation of a fixed burden of existing mutations [13, 22-
175 24] but neglected the input of new mutations during PGC proliferation and oocyte
176 maturation, as well as the loss of germ cells during late gestation. The analysis here shows
177 the importance of considering these additional processes governing the population of
178 mitochondria in germline development.
179
180 **Germline bottleneck increases variance but introduces more *de novo* mitochondrial**
181 **mutations**
182
183 The effect of a bottleneck was assessed in the model by allowing b extra rounds of cell
184 division without mitochondrial replication during early embryonic development (e.g., two
185 extra rounds shown in **Figure 2A**). Each additional cell division leads to an average reduction
186 of $(0.5)^b$ mitochondria in PGCs compared to the base model. For simplicity we then hold
187 mitochondrial numbers at this lower value through the period of PGC proliferation. This
188 assumption gives greater impact to the bottleneck and is consistent with some views [18].

Tighter bottlenecks at this early developmental stage generate greater segregational variance in mutation load between cells (**Figure 2B**). This increase in variance persists and is enhanced through PGC proliferation to the production of primary oocytes and ultimately in mature oocytes (**Figure 2B**). The bottleneck not only creates a wider spread of mutation number per cell, but also the possibility that cells can be mutation free even when initiated from a zygote that contains significant numbers of mutations (**Figure 2B**). Bottlenecks in themselves do not change the mean mutation load, as they occur before the start of mitochondrial replication (i.e. at PGC specification; **Figure 2B**) [55]. But oocyte maturation requires the expansion of mitochondrial number back to half a million. Cells starting with lower numbers must therefore undergo more rounds of mitochondrial replication, and hence will accumulate more *de novo* mutations. So, the mean mitochondrial mutation load in mature oocytes increases with tighter bottleneck size, albeit this effect is small with standard mutation rates ($\mu = 10^{-8}$; **Figure 2B**). Nonetheless, the tension between variance and mean determines the overall selective consequence of the bottleneck.

The advantage that the bottleneck brings depends on how selection acts against the mutation load carried by an individual. Based on the observed dependence of mitochondrial diseases on mutation load [60-62], in which more serious phenotypes typically manifest only at high mutation loads of >60 % [60-62], it is thought that individual fitness is defined by a concave fitness function, indicative of negative epistasis (**Figure 2C**). This assumes that each additional mitochondrial mutation causes a greater reduction in fitness beyond that expected from independent effects. In other words, low mutation loads have a relatively trivial fitness effect, whereas higher mutation loads produce a steeper decline in fitness.

213 The change in mutation load (Δm) over a single generation after individual selection was
214 measured against 5 mean bottleneck sizes ($\bar{B} = 128, 64, 32, 16, 8$), for three initial mutation
215 loads (m_0) and three mutation rates (μ). The bottleneck shows an ambiguous relationship
216 with fitness, dependent on the inherited mutation load (m_0). For the estimated mutation
217 rate ($\mu = 10^{-8}$) there is always an increase in mutation load in individuals who inherit low
218 or medium mutation loads ($m_0 = 0.001, 0.01$; **Figure 2D**). This increase in load ($\Delta m > 0$)
219 becomes more deleterious with a tighter bottleneck (**Figure 2D**). The bottleneck only
220 confers a benefit ($\Delta m < 0$) among individuals who inherit a high mutation load ($m_0 = 0.1$;
221 **Figure 2D**), where the advantage of greater variance outweighs the increase in *de novo*
222 mutation load. If the mutation rate is lower ($\mu = 10^{-9}$), bottlenecks have little effect except
223 when severe, where they again cause an increase in mutation number in individuals with
224 low or medium mutation loads ($m_0 = 0.001, 0.01$; **Figure 2 – figure supplement 1A**). In
225 individuals with high mutation load ($m_0 = 0.1$) only tighter bottlenecks ($\bar{B} = 16, 8$) are
226 beneficial (**Figure 2 – figure supplement 1A**). If the mutation rate is higher ($\mu = 10^{-7}$) the
227 pattern is more extreme, with the accumulation of *de novo* mutations except in individuals
228 with high inherited mutation loads ($m_0 = 0.1$) at the tightest bottleneck size ($\bar{B} = 8$)
229 (**Figure 2 – figure supplement 1B**). In sum: even though bottlenecks generate greater
230 variance, they impose the need for additional rounds of mitochondrial replication during
231 oocyte maturation, resulting in greater *de novo* mutational input. This makes tight
232 bottlenecks advantageous only for rare individuals who inherit high mutation loads, but not
233 for the great majority of the population where the prevalence of mitochondrial mutations is
234 below the limits of detectability, between 0.001 and 0.01 [4, 14].
235

Follicular atresia cannot be explained by realistic selection against cells with high mitochondrial mutation loads

In the analysis of bottlenecks above, the culling of ~8 million oogonia to 1 million primary oocytes at the end of PGC proliferation was assumed to be a random process (**Figure 2A**). This loss has a minimal effect on the mean and variance of mitochondrial mutations in germ cells, given the large numbers involved (and no effect at all when averaged over a population). However, the loss of ~80% of oocytes via follicular atresia during late gestation has long been puzzling and could arguably reflect selection against cells with higher mutation loads.

To analyse follicular atresia, cell-level selection was applied to oogonia at the end of PGC proliferation (**Figure 3A**). PGCs vary in mutation frequency due to both the random segregation of mutants during the multiple cell divisions of proliferation and the chance input of new mutations during mtDNA replication. In principle, we assume that between-cell selection is governed by a negative epistatic fitness function (**Figure 3B**) similar to that thought to apply at the individual level, and vary selection from linear ($\xi = 1$), weak ($\xi = 2$) to strong epistasis ($\xi = 5$). Positive epistasis ($\xi < 1$), whereby a single point mutation produces a steep loss of fitness, but additional mutations have less impact (i.e. mutations are less deleterious in combination), seems biologically improbable, so we do not consider it here.

The effect of cell selection during follicular atresia was calculated as the change in mutation frequency for individuals carrying different mutation loads (m_0) over a single generation,

given standard values for *de novo* mutations ($\mu = 10^{-8}$) and bottleneck size ($\bar{B} = 128$). Under strong negative epistasis ($\xi = 5$), only the few cells with very high mutation loads (generated by segregation) are eliminated. Cell-level selection does not reduce mutation load, even for individuals with a high initial frequency of mutations ($m_0 = 0.1$; **Figure 3C**). Cell-level selection is more effective with weak epistasis ($\xi = 2$) or linear selection ($\xi = 1$) as this makes cells with lower mutation loads more visible to selection, and has a greater benefit in individuals carrying higher initial mutation loads (**Figure 3C**). However, in individuals who inherit low or medium mutation load ($m_0 = 0.001, 0.01$) cell selection offers a minimal constraint against mutation input. The only case in which cell selection produces a benefit is with high mutation load ($m_0 = 0.1$) under linear selection ($\xi = 1$) (**Figure 3C**). This pattern holds for a lower mutation rate ($\mu = 10^{-9}$; **Figure 3 – figure supplement 1A**), while there is no benefit at all at a higher mutation rate ($\mu = 10^{-7}$; **Figure 3 – figure supplement 1B**).

The Balbiani body pools high-quality mitochondria and restricts *de novo* mutation input

An alternative interpretation of atresia in late gestation lies in the formation of the Balbiani Body. We model the developmental process giving rise to the Balbiani body by assuming that cysts of 8 oogonia form at the end of PGC proliferation (**Figure 4A**). Cells within a cyst are derived from a common ancestor (i.e. via 3 consecutive cell divisions). At the 8-cell stage, intercellular bridges form between the oogonia. These allow cytoplasmic transfer of a proportion of mitochondria (f) from each cell to join the Balbiani body of the single cell destined to become the primary oocyte (**Figure 4A**). The mitochondria that undergo cytoplasmic transfer are sampled at random (without replacement), with different weights for wildtype (p_{wt}) and mutant (p_{mut}) mitochondria, until f have moved to the Balbiani

body. The oogonia that donate their cytoplasm to the primary oocyte are now defined as nurse cells, and undergo programmed cell death – atresia (**Figure 4A**).

The model shows that two benefits accrue from cytoplasmic transfer. The first benefit of mitochondrial transfer into the Balbiani body is that pooling increases the number of mitochondria in primary oocytes. As the proportion of mitochondria transferred increases towards the estimated rate of f = 50% [41], the number of mitochondria in primary oocytes increases 4-fold. Pooling therefore cuts the number of rounds of replication needed to reach the extreme ploidy required by mature oocytes, which decreases the input of new mutations from replication errors during oocyte maturation. This benefit accrues whatever the initial mutation load, and more dramatically with a higher mutation rate (**Figure 4 – figure supplement 1**).

The second benefit arises from selective transfer of mitochondria. Preferential exclusion of mutant mitochondria ($p_{wt} > p_{mut}$), as suggested by experimental evidence [41, 51, 63], lowers the mutation load in primordial oocytes (**Figure 4B**). The difference between p_{wt} and p_{mut} determines the extent to which the mutation load is reduced, with stronger exclusion of mutant mitochondria (lower p_{mut}) reducing the number of mutations when the inherited load is medium or high ($m_0 = 0.01, 0.1$), albeit with a negligible effect at low initial mutation load ($m_0 = 0.001$; **Figure 4C**). The same effect is seen with lower and higher mutation rates (**Figure 4 – figure supplement 2**). Nurse cells retain a higher fraction of mutant mitochondria but undergo apoptosis, removing mutants from the pool of germ cells, and explaining the need for an extreme loss of germ cells during late gestation. This effect acts in concert with pooling leading to a reduction in both the mean and variance of

mitochondria mutation load in the cells destined to develop into mature oocytes. (**Figure 4B**).

Evolutionary model

The computational model discussed above gives an indication of the effectiveness of selection at the level of individuals, cells or mitochondria in eliminating mitochondrial mutations across a single generation. To address the long-term balance of mutation accumulation versus selection over many generations, we developed an evolutionary model. This assesses the effectiveness of the three representations of germline development in explaining the observed prevalence of mitochondrial mutation load and disease in human populations (see **Materials and Methods**). This evolutionary model evaluates long-term evolutionary change in an infinite population with non-overlapping generations and is implemented using a number of approximations, which greatly reduce the model complexity (see **Materials and Methods**).

By iterating the patterns of germline inheritance and selection, the equilibrium mutation distribution was calculated across a range of mutation rates and bottleneck sizes. The accuracy of the three models was then assessed as the likelihood of reproducing the observed levels of mitochondrial mutations in the human population (**Figure 5**). Specifically, we used estimated values of 1/5000 for mitochondrial disease (>60% mutant), 1/200 for carriers of mitochondrial mutants (2-60% mutant) and hence 99.5% of individuals are 'mutation free' (i.e. carry <2% mutants, the threshold for detection in these estimates of mutation frequency [4, 5]). Recent deep-sequencing estimates using a mutation detection threshold of >1% [14], show that a minor allele frequency of 1-2% is relatively common in

selected human PGCs, but this does not alter earlier population-level estimates of the proportion of carriers not suffering from overt mitochondrial disease, defined as a 2-60% mutation load used here.

Likelihood heatmaps confirm that selection at the level of individuals or cells alone do not readily approximate the clinical data whatever the bottleneck size (**Figure 5A-B**). Only at a mutation rate $\mu < 0.5 \times 10^{-8}$ do these forms of selection offer explain the observed mutation load and disease frequency in humans at high likelihood, especially when using tighter bottlenecks (**Figure 5A**). These limitations do not apply to the preferential transfer of wildtype mitochondria into the Balbiani body (**Figure 5C-D**). Even intermediate levels of selection against the transfer of mutant mitochondria into the Balbiani body ($p_{mut} = 0.33$, $p_{wt} = 0.67$) generates a high log-likelihood of reproducing the clinical data at the standard mutation rates ($\mu = 10^{-8}$) and bottleneck sizes (> 100 mitochondria per cell) (**Figure 3C**). Stronger selection on transfer probabilities ($p_{mut} = 0.25$, $p_{wt} = 0.75$) can account for the clinical pattern under a wide range of bottleneck sizes and mutation rates (**Figure 5D**).

DISCUSSION

How selection operates on mitochondria has long been controversial. At the heart of this problem is the paradox that mtDNA accumulates mutations faster than nuclear genes, yet there is evidence that mtDNA is under strong purifying selection. Mitochondrial mutations accumulate through Muller's ratchet, as mtDNA is exclusively maternally inherited, and does not undergo recombination through meiosis [3]. In addition, mitochondrial genes are highly polyploid, which obscures the relationship between genotype and phenotype,

hindering the effectiveness of selection on individuals. Despite these constraints, deleterious mitochondrial mutations seem to be eliminated effectively [6-11], facilitated by female germline processes that have long been mysterious. These include: the excess proliferation of primordial germ cells (PGCs) [64]; the germline mitochondrial bottleneck (when mitochondrial numbers are reduced to a disputed minimum in PGCs) [13-15]; the formation of the Balbiani body in primary oocytes [41, 51]; the atretic loss of 70-80% of germ cells during late gestation [31, 39]; the extended oocyte quiescence until puberty or later (during which time mitochondrial activity and replication is suppressed) [58, 65]; and the generation of around half a million copies of mtDNA in mature oocytes [59]. The key question is how do these processes facilitate the maintenance of mitochondrial quality over generations?

In this study, we introduced a computational model that considers these germline processes from the perspective of mitochondrial proliferation, segregation and selection, using realistic estimates of parameter values, drawn from the human literature [29, 55]. Most work to date [13, 15-18] has focused on the mitochondrial bottleneck as a means of generating variation in mitochondrial content between oocytes and by extension zygotes (**Figure 2B**), furnishing the opportunity for selection to act on individuals in the following generation. These studies have been unable to reconcile serious differences in experimental estimates of mitochondrial numbers during PGC proliferation, inciting inconclusive debates over the tightness of the bottleneck [13, 15-18]. More significantly, this earlier work neglects an important germline feature, the introduction of *de novo* mitochondrial mutations produced by copying errors [66] rather than damage by reactive oxygen species [57, 67]. These accumulate during PGC proliferation and, equally importantly, during the

mass-production of mtDNAs in the mature oocyte. Tighter bottlenecks are disadvantageous as they impose the need for more rounds of mitochondrial replication which means a greater input of *de novo* mutations. Our modelling shows that for most individuals the mean mutation load shows little meaningful change (**Figure 2D**), regardless of whether the mutation rate is set low or high (**Figure 2 – figure supplement 1**), and in fact increases with tighter bottleneck size (**Figure 2D**). Most individuals have low mutation loads (~99.5% in human populations [4, 5]), and for them, the normal process of repeated segregation during cell division generates sufficient variance in itself. Any marginal increase in variance caused by bottlenecks is more than offset by increased mutational input. Tighter bottlenecks only benefit individuals who already carry high mutation loads (i.e. $m_0 \geq 0.1$, **Figure 2D**). For them, there is benefit in further reductions in bottleneck size as this increases the fraction of mature oocytes with significantly reduced mutation load (**Figure 2D**). In the modelling, we assumed that the bottleneck size was maintained across the period of PGC proliferation. Some studies have found that from a low number in early development, copy number increases 5-10 fold to production of the oogonia [16, 17]. This would lessen the effect of the bottleneck in general as it would have less effect on segregation.

These results show that the popular idea that a germline mitochondrial bottleneck facilitates selection against mitochondrial mutations is misconstrued. The value of a bottleneck depends on the unforeseen trade-off between increasing genetic variance and mutation input. In fact, the reduction in mitochondrial copy numbers from zygote to primordial germ cells should be thought of as the reestablishment of a typical copy number at the start of cellular differentiation, which commences after multiple cell divisions *without* mtDNA replication. What counts as a bottleneck are the 'extra' rounds of cell division

reducing mitochondrial number below the 'normal' number, and the incremental increase in variance this induces. Most critically, the bottleneck needs to be understood in relation to oogamy, the massively exaggerated mitochondrial content of the female gamete. This is a characteristic of metazoan gametogenesis [59]. Previous work has shown it is beneficial in animals with mutually interdependent organ systems [59]. The extreme ploidy in the zygote allows early rounds of cell division to occur without mitochondrial replication, and hence without *de novo* mutational input. These initial cell divisions generate little between-cell differences, as segregational variance is weak when numbers are high and mitochondria segregate randomly during mitosis [52] (e.g. **Fig 1B** before PGC specification). So at the point of cellular differentiation (~12 cell divisions) there is homogeneity in the mutation load among the different organ systems and no one system is likely to fail, which would massively lower the fitness of the whole organism [59]. This contrasts with organisms that have modular growth, such as plants and morphologically simple metazoa (sponges, corals, placozoa), which neither sequester a recognizable germline distinct from the stem-cell lineage early in development (although recent work challenges this view), nor have oocytes with massively expanded mitochondrial numbers [56, 59, 68-70].

Follicular atresia is another female germline feature examined in our modelling, in which there is over-proliferation of PGCs followed by ~80% loss early in development, before oocyte maturation [31, 39]. This massive reduction in germ cell number has long been enigmatic. It is unlikely to be random, yet does not obviously serve a selective function, as it seems unlikely that such a high proportion of germ cells could have low fitness [26-28]. The model confirms this intuition. Selection among PGCs at the end of the period of proliferation has little effect in significantly reducing mutation load (**Figure 3C**). Assuming a

concave fitness function (**Figure 3B**), which seems reasonable by extension from the severity of mitochondrial diseases [60, 62], between-cell selection is ineffective, as it only eliminates PGCs with very high mutational numbers. This has little effect in constraining the burgeoning of lower mutation loads. Linear selection does better, even if it seems unrealistic, as it will act against a broader range of mutational states. But as with bottlenecks, it is only beneficial in individuals already carrying significant mutation loads (i.e. $m_0 \geq 0.1$, **Figure 3C**). We conclude that cell-level selection produces little measurable reduction in mutation load and so is unlikely to be responsible for follicular atresia.

A more recent explanation of PGC loss relates to the formation of the Balbiani body in primary oocytes [41, 44]. In many metazoa, including clams [46], insects [45, 71], mice [49] and probably humans [44], the over-proliferation of PGCs culminates in their organization into germline cysts of multiple oogonia connected by cytoplasmic bridges [41, 49, 71]. These connections are thought to allow the transfer of mitochondria and other cytoplasmic constituents by active attachment to microtubules, into what becomes the primary oocyte [41]. The surrounding oogonia that transferred their mitochondria, now termed nurse cells, die by apoptosis [41]. The plethora of terms should not mask the key point that nurse cell death accounts for a considerable fraction of the germ cell loss usually ascribed to follicular atresia. We modelled selective mitochondrial transfer into the Balbiani body, perhaps in part reflecting membrane potential [45, 51]. This achieves two complementary benefits: it purges mutations and pools high-quality mitochondria in a single cell. If the germline cyst is composed of eight cells that contribute half of their mitochondria to the Balbiani body, then the primary oocyte gains four times as many mitochondria which have passed through quality control. This also cuts the need for additional rounds of mtDNA copying, and so

reducing the input of *de novo* mutations. Selective transfer and pooling lowers the mutation load across a wide range of mutation rates and inherited loads (**Figure 4C, Figure 4 – figure supplement 1-2**). This process differs from mitophagy, the main route used in somatic cells for maintaining mitochondrial quality [72, 73], as it not only removes mutant mitochondria, but crucially also increases mitochondrial numbers, a key requirement for prospective gametes. The requirement for pooling of mitochondria to lower the mutation load from copying errors also aligns with experimental observations of active spindle-associated mitochondrial migration to the generative oocyte in the formation of polar bodies during meiosis I of oogenesis [74]. We predict that selection for mitochondrial quality occurs during this process (i.e. polar bodies retain mutant mitochondria) but have not dealt with that explicitly in the model.

These insights depend in part on the parameter values used in the modelling, many of which are uncertain. We have examined variation around the most representative values drawn from the literature [2, 14, 75, 76], and aimed to be conservative wherever possible. We considered mutation rates across two orders of magnitude, around 10^{-8} per bp as the standard [75] and a similar range of bottleneck sizes ($\bar{B} = 8 - 128$). Strong selective pooling of mitochondria into the Balbiani body predicts the observed prevalence of mitochondrial mutations and diseases in human populations [4, 5] under a wide range of mutation rates and bottleneck sizes (**Figure 5**). Selection at the level of individuals or cells are much more constrained explanations, although we do not rule out some role for these processes (**Figure 5**). In general, higher mutation rates (10^{-7} per base pair) strengthen the conclusions discussed here (**Figures 2-4 – figure supplement 1-2**) whereas the lowest mutation rates are more commensurate with weaker forms of evolutionary constraint generated by selection

476 on individuals or cells. Plainly, weaker selection approximates best to clinical data when the
477 mutation input tends towards zero (**Figure 5**). However, such low mutation rates are not
478 consistent with the 10-30-fold faster evolution rates of mtDNA compared with nuclear
479 genes [1, 2], or with the strong signatures of purifying [6] and adaptive [7] selection on
480 mitochondrial genes. In the modelling, we ignored the contribution of oxidative damage
481 caused by reactive oxygen species. While this source of mutation is likely low compared
482 with copying errors [57, 66], oxidative mutations may accumulate over female reproductive
483 lifespans [67], perhaps contributing to the timing of the menopause [77]. As primary
484 oocytes contain ~6000 mitochondria [77], expansion up to ~500,000 copies in the mature
485 oocyte will amplify any mutations acquired during oocyte arrest at prophase I, potentially
486 over decades [66]. The metabolic quiescence of oocytes can best be understood in light of
487 the need to repress mitochondrial mutation accumulation during the extended period
488 before reproduction [58, 65].
489
490 We have addressed here a simple paradox at the heart of mitochondrial inheritance. Like
491 Gibbon's *Decline and Fall of the Roman Empire*, mitochondrial DNA is often portrayed as
492 being in continuous and implacable decline through Muller's ratchet [3]; yet like the Empire,
493 which endured for another millennium, mitochondrial DNA has persisted and has been at
494 the heart of eukaryotic cell function for over a billion years [78]. Strong evidence for
495 purifying and adaptive selection implies that the female germline facilitates selection for
496 mitochondrial quality, but the mechanisms have remained elusive. We have modelled
497 segregation and selection of mitochondrial DNA at each stage of germline development, and
498 shown that direct selection for mitochondrial function during transfer into the Balbiani body
499 is the most likely explanation of the observed prevalence of mitochondrial mutations and

diseases in human populations. More remarkably, this mitochondria-centric model elucidates the complexities of the female germline. It explains why mature oocytes are crammed with mitochondria [59], whereas sperm mitochondria are typically destroyed, giving rise to two sexes [25]; why germ cells over-proliferate during early germline development; why oogonia organize themselves into germline cysts, forming the Balbiani body; why the majority of germ cells then perish by apoptosis as nurse cells; why primary oocytes enter metabolic quiescence, sometimes for decades; and even why polar bodies channel most of their mitochondria into a single mature oocyte. The need for mitochondrial quality extends to somatic cells, as mitochondria activity is crucial to cellular, tissue and organ functioning in the adult organism [79-81]. Some of the approaches we have adopted here need to be applied to development and whether specific processes have evolved to maintain mitochondria where their function is more critically related to somatic fitness [59, 82]. Most fundamentally, this perspective challenges the claim that complex multicellularity requires passage through a single-celled, haploid stage to constrain the emergence of lower-level, selfish genetic elements [82, 83]. This is true for nuclear genes in oocytes, whose quality is maintained by sexual exchange and recombination [83], but is not the case for mitochondria, which are generally transmitted uniparentally, without sexual exchange or recombination. In animals, the oocyte cytoplasm is not derived from a single cell, but instead requires the selective pooling of mitochondrial DNA from clusters of progenitor cells, which together generate high-quality mitochondria at extreme ploidy in mature gametes.

MATERIALS AND METHODS

Computational Model

1. Initial conditions

We use a computational model implemented in MATLAB (**RRID:SCR_001622**) to follow the distribution of mitochondrial mutations in the female germline over a single generation from zygote to a new set of mature oocytes, as set out in the developmental history given in the main text (**Figure 1A**). The initial state of the system is a zygote containing $M_0 = 2^{19} = 524{,}288$ copies of mtDNA [59, 84], of which m_0 carry a deleterious mutation. Three specific models are considered: bottleneck, follicular atresia and cytoplasmic transfer. A list of terms and parameter values is given in **Table 1**, which also apply in the evolutionary model considered below.

Table 1

Parameters and variables	Symbols and values
Maximum number of germ cells	$N_{max} = 8{,}388{,}608$
mtDNA number in mature oocytes	$M_0 = 2^{19} = 524{,}288$
Minimum mtDNA ploidy	B
Final number of germ cells	$N_{max}/8 = 1{,}048{,}576$
Initial mutation load	m_0
Mutation rate per bp per cell division	μ
Strength of epistatic interactions	ξ
Transfer probability of mutant mtDNA	p_{mut}
Transfer probability of wildtype mtDNA	p_{wt}
Human mitochondrial genome size	$g = 16{,}569$bp [85]

2. Early embryonic development

During early embryonic development, there is no mtDNA replication. The number of cells doubles at each time step. The existing population of mutant and wildtype mtDNA undergoes random segregation into daughter cells according to a binomial distribution – each mtDNA copy has a 50% probability of being assigned to either daughter cell. During this process, the average number of mtDNA copies per cell halves at each time step. There is no mutational input, as we only consider mutations that arise due to replication errors.

3. PGC proliferation, oogonia cell death and oocyte maturation

The early embryonic period lasts for the first 12 cell divisions. A group of 32 cells is selected at random to form the primordial germ cells (PGC). The PGCs then undergo proliferation for a further 18 rounds of cell division, until the maximum number of germ cells is reached, $N_{max} = 32 \times 2^{18} = 8{,}388{,}608$. This value is close to the average reported in the literature [29].

mtDNA replication resumes after cell division 12, at the point of PGC determination. At this point, cells have an average of 128 mtDNA copies. At each following time step, the number of mtDNA copies doubles prior to random segregation into daughter cells. This means that the average number of mtDNA copies per cell is kept constant. New mutations are introduced as errors in mitochondrial replication. During the replication process, the new replica of each wildtype mtDNA copy has a probability of mutation μ/bp. The genome wide mutation rate $U = g \times \mu$ is calculated as genome size ($g = 16{,}569$ bp [85]) multiplied by μ. This estimate assumes each site contributes equally to selective effects and ignores many subtleties relating to mutation probability and within-cell maintenance processes, but

should give a reasonable order of magnitude gauge of the target size of mutational input per cell division. Given n wildtype and m mutant mtDNAs, the number of new mutants Δm resulting from replication errors is obtained by sampling at random from a binomial distribution with n trials with probability U. After replication and mutation and prior to segregation the total number of wildtype and mutant mtDNAs is $2n - \Delta m$ and $2m + \Delta m$ respectively. Back mutation to wildtype is not permitted.

At the end of PGC proliferation, the N_{max} oogonia undergo random cell death, leaving $N_{max}/8 = 1{,}048{,}576$ primary oocytes. This is achieved by sampling the surviving cells at random with uniform weights (i.e., every cell has an equal probability of survival). The primary oocytes do not undergo further cell division or mitochondrial replication during the quiescent period (this is not explicitly modelled). At puberty, oocyte maturation commences. The number of mitochondria per cell is brought back to the original value $M_0 = 2^{19}$ through 12 rounds of replication without cell division. We assume that the number of mtDNA copies doubles at each time step. This introduces new deleterious mutations, which again are randomly drawn from a binomial distribution (as described above).

4. Specific models of selection

We consider three specific models in the main text with modifications to the base model described above.

The first model adds a bottleneck stage at the time of PGC determination (**Figure 2**). As before, 32 cells are selected at cell division 12 to form the PGCs. These go through b extra

584 rounds of cell division without mtDNA replication. This reduces the mean number of mtDNA
585 copies per cell to $\bar{B} = 128 * (0.5)^b$. The mtDNA replication commences at cell division 14.
586 The PGCs then proliferate as before to produce oogonia that undergo random cell death to
587 produce primary oocytes. The primary oocytes have a reduced number of mtDNA copies,
588 and so must undergo $12 + b$ extra rounds of mtDNA replication in order to regain the
589 original value M_0 mitochondria in mature oocytes. Note that this is an extreme model of the
590 bottleneck, where mtDNA copy number is kept low throughout the period of PGC
591 proliferation, and so maximises the benefit derived from the increase in segregational
592 variation caused by the bottleneck.
593
594 For the model of the bottleneck, we allow selection dependent on individual fitness in
595 relation to their mutation load m among mature oocytes, according to the fitness function
596 $f(m) = 1 - (\frac{m}{M})^5$ (**Figure 2C**). The concave shape of this function accounts for the fact that
597 mitochondrial mutations typically have a detrimental effect on individual fitness only for
598 loads >60%. Changes to the power exponent make little qualitative difference to the
599 outcome of this model (data not shown).
600
601 A second model considers non-random death during the cull of oogonia as these cells
602 transition to being primary follicles (**Figure 3**). Selection in this case is applied at the cell
603 level. Cell fitness is expressed as $f(m) = 1 - (\frac{m}{M})^{\xi}$, where m is the number of mutant
604 mitochondria. The parameter ξ determines the strength of epistatic interactions (**Figure**
605 **3B**). As in other models, the number of cells is reduced from $N_{max} = 8{,}388{,}608$ to
606 $N_{max}/8 = 1{,}048{,}576$. This is achieved by sampling without replacement the surviving cells

607 at random, with weights proportional to cell fitness (i.e., every cell has a probability of
608 survival proportional to its fitness).
609
610 The third model considers that the oogonia are organised in cysts of 8 cells each. These are
611 the descendants of a single cell (*i.e.* three cell divisions prior). One cell is randomly
612 designated as the primary oocyte using the MATLAB function randsample. The Balbiani body
613 of the primary oocyte contains a proportion f of the mtDNA copies of all cells in the cyst.
614 The mitochondria that join the Balbiani body are sampled at random without replacement
615 from each cell with different weights for wildtype (p_{wt}) and mutant (p_{mut}). After
616 mitochondrial transfer to the Balbiani body, nurse cells undergo apoptosis (i.e. all cells
617 except the one designated as the primary oocyte), reducing the total number of oocytes to
618 $N_{max}/8 = 1{,}048{,}576$.
619
620 **Evolutionary Model**
621 In order to calculate the equilibrium distribution of a population undergoing the
622 developmental dynamics mentioned in the previous section, we develop an analytical
623 model for the distribution of mitochondrial mutations in an infinite population, with non-
624 overlapping generations. As it was not possible to find an analytical solution, we solved the
625 equations through numerical iterations. The system converges to a unique equilibrium
626 state, independent of the initial conditions.
627
628 The state of the system is described by the vector $p(t) = \{p_0(t), \dots, p_{M(t)}(t)\}$, where
629 $M(t)$ is the number of mtDNA copies per cell at time t. The elements $p_m(t)$ are the
630 frequency of mutation load $m(t)/M(t)$ at time t. The evolution of the system is determined

631 by a set of transition matrices whose elements are the transition probabilities between
632 states. To avoid unnecessary complexity in the evolutionary model, we assume that
633 fluctuations in mitochondrial number per cell due to segregation are negligible (*i.e.* in
634 contrast to the computational model which allows binomial segregation at each division).
635 Therefore, the mtDNA number per cell is constant across the whole population of cells at
636 every time step. That is, during early embryonic development (when there is no mtDNA
637 replication), after t cell divisions, the total number of mitochondria per cell is $M^{(t)} =$
638 $2^{-t}M_0$. Then, during PGC proliferation, the total number of mitochondria per cell is
639 constant. Finally, during oocyte maturation, the number of mitochondria per cell exactly
640 doubles with each mtDNA replication cycle. To aid in calculations, we also set the initial
641 number of mtDNA copies to be proportional to the bottleneck size, *i.e.* $M_0 = 2^{12} \times B$. As
642 the mtDNA number per cell halves at each cell division during early embryonic
643 development, setting M_0 this way allows the mtDNA number to remain an integer. This is
644 important for the modelling procedure, because the dimension of the transition matrixes
645 (which is determined by the mtDNA number) must be an integer.
646
647 1. Early embryonic development
648 During early embryonic development, when mitochondrial replication is not active, changes
649 in frequency arise purely from the process of segregation. Let $W^{(t)}$ be a $M^{(t)} + 1 \times M^{(t)} +$
650 1 square matrix, whose elements W_{mn} represent the transition probabilities from a state
651 with m to a state with n mutants:

$$W_{mn}^{(t)} = \binom{m}{n}\binom{M^{(t-1)} - m}{M^{(t)} - n} \Big/ \binom{M^{(t-1)}}{M^{(t)}} \quad (1)$$

652

These matrix elements model the probability of transitioning from a state with m mutants and $M-m$ wildtype to a state with n mutants and $M-n$ wild type via the segregation of $2M$ mitochondria into two daughter cells with M mitochondria each.

After t cell divisions, the average number of mutants per cell is $\overline{m} = 2^{-t} m_0$, and the variance is $Var(t) = \frac{1}{4}[Var(t-1) + 2^{-t} m_0]$. The state of the system is updated as $\vec{p}^{(1)} = \left(\prod_t W^{(t)}\right) \times \vec{p}^{(0)}$.

2. PGC proliferation, oogonia cell death and oocyte maturation

During PGC proliferation, new mutations are introduced at a rate $U = \mu \times g$. The transition coefficient Q_{mn} from a state with m to a state with n mutants results from the combined effects of replication, mutation and segregation:

$$Q_{mn} = \sum_k \binom{M-n}{k-n} U^{k-n} (1-U)^{M-k} \binom{k}{m} \binom{M-k}{M-m} \Big/ \binom{2M}{M} \qquad (2)$$

$$= \sum_k \binom{M-n}{k-n} U^{k-n} (1-U)^{M-k} a_{k,m}$$

The coefficient $a_{k,m} = \binom{k}{m}\binom{M-k}{M-m}/\binom{2M}{M}$ models the probability of transitioning from a state with k mutants and $M-k$ wildtype to a state with n mutants and $M-n$ wild type via the segregation of $2M$ mitochondria into two daughter cells with M mitochondria each; the remaining part of the equation models the probability of reaching a state with k mutant mitochondria through replication and mutation of M mitochondria, of which m are mutant (this corresponds to the probability of introducing $k-m$ new mutations). The system is

672 updated $\vec{p}^{(2)} = Q^q \times \vec{p}^{(1)}$, across q rounds of PGC cell division. We then apply particular
673 processes to capture the effects of the bottleneck, follicular atresia and cytoplasmic
674 transfer.
675
676 As before, we model the bottleneck as b extra rounds of segregation before the onset of
677 mtDNA replication, following **Eq(1)** with $q + b$ cell divisions. This has no effect on the mean
678 mutational number but increases mutational variance between the resulting PGCs. The
679 transition between oogonia and primary oocytes occurs at random, and so does not alter
680 the frequency distribution of mutants. Finally, during oocyte maturation, the mtDNA
681 content of each cell doubles at every time step until the initial ploidy M_0 is restored. The
682 transition matrix G_{mn} is analogous to the first term of **Eq(2)**, incorporating replication and
683 mutation, but without segregation (last term of **Eq(2)**):
684

$$G_{mn}^{(t)} = \binom{M^{(t)} - m}{n - m} U^{n-m} (1 - U)^{M-k} \quad (3)$$

685 **Eq(3)** models the probability of transitioning from a state with m to a state with n mutants,
686 which is equivalent to the probability that exactly $n - m$ out of $M^{(t)} - m$ wildtype acquire a
687 deleterious mutation. As the bottleneck reduces mtDNA copy number per cell, there is the
688 need for b extra rounds of replication of mtDNA during oocyte maturation. Hence, the
689 transition coefficient G is applied $b + 12$ times in the bottleneck model, to restore the
690 number of mtDNA copies per oocytes to the original ploidy level M_0: $\vec{p}^{(3)} = \left(\prod_t G^{(t)}\right) \times$
691 $\vec{p}^{(2)}$.
692

693 At the end of the maturation phase, for the bottleneck model, selection is applied on
694 individual fitness using a vector w whose elements w_m are equal to the corresponding
695 fitness: $w_m = f(m) = 1 - \left(\frac{m}{M}\right)^5$. This causes a change in the population mutation load as
696 the system is updated to:

$$\vec{p}^{(3)} = (I\vec{w})\,\vec{p}^{(2)}/\vec{w}^T\,\vec{p}^{(2)} \quad (4)$$

697 where I is the identity matrix.
698
699 In the model of follicular atresia, an extra step is included to reflect selection that operates
700 when the population of oogonia are culled to produce the primary oocytes. This causes a
701 change in the population mutation load analogous to that described in **Eq(4)**, but using the
702 cell fitness function $w_m = f(m) = 1 - \left(\frac{m}{M}\right)^{\xi}$ instead. This determines the shift in mutation
703 loads that arises from fitness-dependent culling of oogonia. The transition coefficient **Eq(3)**
704 for oocyte maturation is then applied 12 times in the follicular atresia model, to restore the
705 original level of ploidy.
706
707 Finally, in order to model cytoplasmic transfer, a different process is used in the production
708 of primary oocytes. A set of 8 clonally derived cells is selected. The mutation levels of each
709 cell in the cyst is obtained by applying **Eq(3)** three times. Then, 50% of the mitochondria in
710 each cell are pooled into the Balbiani body of the primary oocyte. The probability for a cell
711 with m mutants to contribute n mutants to the Balbiani body is given by:

$$C_{nm} = \binom{m}{n} p_{mut}^{n} \binom{M-m}{M/2-n} p_{wt}^{M/2-n} \; /N \quad (5)$$

712

Which gives the number of permutations of n mutant and $M/2 - n$ wildtype mtDNA copies, weighted by the probability of transfer $p_{mut}$and p_t respectively, and divided by a normalisation constant N. As the primary oocyte contains half of mitochondria from 8 cells, it needs to undergo 2 fewer rounds of replication during oocyte maturation. Hence only 10 rounds of replication following **Eq(3)** are carried out in this case to restore the original level of ploidy.

For all three models (bottleneck, follicular atresia and cytoplasmic transfer), the frequency distribution of mutation loads after these steps is used as the starting point for the next generation.

3. Evolutionary dynamics and model accuracy

The processes described above are iterated until the Kullback-Leibler divergence (a theoretical measure of how two probability distributions differ from each other [86]) between the new and the old distribution is smaller than a threshold $\eta = 10^{-9}$. We then assume that the system has reached a stationary state, *e.g.* without significant changes in the overall distribution of mutation loads between generations (mutation-selection balance).

In order to compare the prediction of the model with the clinical data, we use the equilibrium distribution to calculate the fraction of the population which carries a detectable load of mitochondrial mutations but does not manifest any detrimental phenotype (α_1) and the fraction of individuals affected by mitochondrial disease (α_2) using a

threshold of 60% mutation load to discriminate between carrier and disease status. Individuals are assumed to be mutation free beyond the detection threshold of 2% [4].

The accuracy of the model is evaluated as the logarithm of the probability of reproducing clinical data by sampling the theoretical distribution at random. This is calculated as follows: let X_1 be the number of healthy individuals with detectable mutation load, and X_2 be the number of individuals affected by mitochondrial diseases; N_1 and N_2 the total number of individuals in the two trials; α_1 and α_2 the probability of observing, respectively, a healthy individual with detectable mutation load and an individual affected by mitochondrial disease, according to the prediction of the model. The log-likelihood of observing X_1 and X_2 by random sampling the theoretical distribution is given by

$$\begin{aligned}\log(\lambda_{tot}(\mu, M, \dots) &= log\left[\prod_{i=1}^{2} p\big(X_i\big|\alpha_i(\mu, M, \dots)\big)\right] \\ &= \sum_{i=1}^{2} \log\left[\binom{N_i}{X_i}\alpha_i^{N_i}(1-\alpha_i)^{N_i - X_i}\right] \\ &= \sum_{i=1}^{2} log\binom{N_i}{X_i} + N_i\alpha_i + (N_i - X_i)(1-\alpha_i)\end{aligned} \tag{6}$$

Estimation of the deleterious mutation rate

The parameter values for the deleterious mutation rate we investigate reflect data collected from a number of species. Estimates of mtDNA point mutation rates in the crustacean *Daphnia pulex* range between 1.37×10^{-7} and 2.28×10^{-7} per site per generation [87]. Assuming this rate applies to humans and there are ~ 20 cell divisions before oocyte

753 maturation, leads to a range between 0.68×10^{-8} and 1.14×10^{-8} per site, per cell
754 division. Analysis of *Caenorhabditis elegans* mtDNA leads to a similar estimate of
755 $\sim 1.6 \times 10^{-7}$ per site, per generation [88], which corresponds to a rate of 0.8×10^{-8} per
756 site, per cell division. For *Drosophila melanoganster*, the mtDNA mutation rate yields an
757 estimate of 6.2×10^{-8} per site, per generation, and hence $\sim 0.31 \times 10^{-8}$ per site, per cell
758 division [89]. Finally, analysis of human mtDNA point mutation rates give a mutation rate of
759 0.0043 per genome per generation [75], corresponding to $\sim 1.3 \times 10^{-8}$ mutations per site,
760 per cell division.
761
762 These values do not take into account the presence of a number of processes likely to
763 remove mutants and is therefore a conservative estimate. The loss of mutations would
764 mean that the actual mutation rate is higher than the estimates above. But unlike nuclear
765 rates, the compact structure of mtDNA where intergenic sequences are absent or limited to
766 a few bases, means that the rate of point mutations is probably not much higher than the
767 rate of deleterious mutations. Therefore, for this study we consider a broad interval of
768 possible deleterious mutation rates, labelled as low (10^{-9}), standard (10^{-8}) and high
769 (10^{-7}).
770

771 **FIGURE LEGENDS**

772

773 **Figure 1**

774 **Stages in female germline development.**

775 (**A**) Timeline of human oocyte development showing the main stages modelled, with
776 wildtype (blue) and mutant mitochondria (orange). (**B**) Numerical simulation of the base
777 model. Top panel: number of germ cells from specification of the 32 primordial germ cells
778 (PGCs) after 12 cell divisions; proliferation to form 8 million oogonia; random cell death
779 reducing to 1 million primary oocytes; quiescent period (not shown) and finally oocyte
780 maturation at puberty. Middle panel: copy number of mitochondria (i.e. mtDNA); from
781 zygote with ~500,000 copies, which are partitioned at cell division during early embryo
782 development until replication begins (first vertical line) during PGC proliferation; copy
783 number is amplified during oocyte maturation back to ~500,000 copies; dotted line shows
784 the mean mitochondria copy number, with the distribution across oocytes shown in yellow.
785 Note, skew reflects the log-scale. Bottom panel: mean (dotted line) and distribution of
786 mutation load through development. The yellow shaded area shows the 90% quantile.
787 Other parameter values $\mu = 10^{-8}$, $m_0 = 0.1$.

788

789 **Figure 2** with 1 supplement

790 **Model of germline bottleneck and individual selection.**

791 (**A**) A bottleneck with two extra rounds of cell division without replication (cell division 13
792 and 14; after the first vertical line), reducing mitochondria copy number per PGC (by a
793 quarter on average). Two extra rounds of mitochondrial replication are required to
794 regenerate the copy number in mature oocytes. Compared to the base model (**Figure 1**),

mean mutation load (dotted line, bottom panel) is slightly higher and variation in load is substantially greater (yellow shaded area, 90% quantile). Parameter values $\mu = 10^{-8}$, $m_0 = 0.1$. (**B**) Violin plots of the distribution of mutations (mean ± SD shown in red) at two developmental stages, PGC specification and mature oocytes, given 5 mean bottleneck sizes ($\bar{B}$) when $m_0 = 0.1$. (**C**) Strength of selection on individual fitness, with a concave fitness function based on clinical data from mitochondrial diseases[27,28]. (**D**) Change in mutation load (Δm) across a single generation for three initial mutation loads (m_0), given 5 mean bottleneck sizes ($\bar{B}$), showing the median (red line) and distribution (box plot IQR with min/max whiskers and outliers).

Figure 2 – figure supplement 1

Bottleneck change in mutation load with different mutation rates.

Change in mutation load (Δm) across a single generation after individual selection with variable mean bottleneck size ($\bar{B}$). This is shown with (**A**) low ($\mu = 10^{-9}$) and (**B**) high ($\mu = 10^{-7}$) mutation rate, for individuals with low ($m_0 = 0.001$), medium ($m_0 = 0.01$) and high ($m_0 = 0.1$) initial mutation loads. Box plots show the median (red line) and distribution (box plot IQR with min/max whiskers and outliers).

Figure 3 with 1 supplement

Model of follicular atresia and cell selection.

(**A**) After PGC proliferation, follicular atresia occurs through selective apoptosis of oogonia. (**B**) Cell fitness is assumed to be linear ($\xi = 1$) or follow negative epistasis ($\xi = 2, 5$) in which mutations are more deleterious in combination. (**C**) Change in mutation load, Δm, across a single generation after cell selection, at an intermediate mutation rate ($\mu = 10^{-8}$),

819 for individuals with low ($m_0 = 0.001$), medium ($m_0 = 0.01$) and high ($m_0 = 0.1$) initial
820 mutation loads, for variable levels of epistasis (median (red line) and distribution (box plot
821 IQR with min/max whiskers and outliers)).
822
823 **Figure 3 – figure supplement 1**
824 **Follicular atresia and cell selection change in mutation load with different mutation rates.**
825 Change in mutation load (Δm) across a single generation after cell selection with variable
826 levels of epistasis (ξ). This is shown with (**A**) low ($\mu = 10^{-9}$) and (**B**) high ($\mu = 10^{-7}$)
827 mutation rate, for individuals with low ($m_0 = 0.001$), medium ($m_0 = 0.01$) and high
828 ($m_0 = 0.1$) initial mutation loads. Box plots show the median (red line) and distribution (box
829 plot IQR with min/max whiskers and outliers).
830
831 **Figure 4** with 2 supplements
832 **Model of cytoplasmic transfer and mitochondria selection.**
833 (**A**) Cytoplasmic bridges form among oogonia in the germline cyst, leading to selective
834 transfer of wild-type mitochondria (blue) to the primary oocyte, leaving mutant
835 mitochondria (red) in nurse cells that then undergo apoptosis. (**B**) Cytoplasmic transfer
836 which selectively pools $f = 50\%$ of mtDNA from 8 germline cyst cells into a single primary
837 oocyte causes a large increase in the number of mitochondria (middle panel) and a large
838 reduction in the mean (dotted line, bottom panel) and distribution of mutation load (yellow
839 shaded area shows the 90% quantile, bottom panel), which persists during oocyte
840 maturation. Pooling of mtDNA requires two fewer rounds of mtDNA replication to
841 regenerate copy number in mature oocytes. Parameter values $\mu = 10^{-8}$, $m_0 = 0.1$. (**C**)
842 Change in mutation load (Δm) across a single generation (median (red line) and distribution

(box plot IQR with min/max whiskers and outliers)), for individuals with low ($m_0 = 0.001$), medium ($m_0 = 0.01$) and high ($m_0 = 0.1$) initial mutation loads, with variable strengths of selective transfer (p_{mut}). Parameter value $\mu = 10^{-8}$.

Figure 4 – figure supplement 1

Cytoplasmic transfer and mitochondria selection change in mutation load with different mutation rates and proportion of transferred mitochondria (f).

Change in mutation load (Δm) across a single generation, given a variable proportion of transferred mitochondria (f) to the Balbiani body when transfer is non-selective ($p_{mut} = p_{wt} = 0.5$). This is shown with (**A**) low ($\mu = 10^{-9}$), (**B**), standard ($\mu = 10^{-8}$) and (**C**) high ($\mu = 10^{-7}$) mutation rate, for individuals with low ($m_0 = 0.001$), medium ($m_0 = 0.01$) and high ($m_0 = 0.1$) initial mutation loads. Box plots show the median (red line) and distribution (box plot IQR with min/max whiskers and outliers).

Figure 4 – figure supplement 2

Cytoplasmic transfer and mitochondria selection change in mutation load with different mutation rates and probability of mutant transfer (p_{mut}).

Change in mutation load (Δm) across a single generation, for individuals undergoing cytoplasmic transfer the Balbiani body with variable strength of selection, given a fixed probability of transfer of wildtype mitochondria ($p_{wt} = 0.5$) and a decreasing probability of transfer of mutant mitochondria (p_{mut}). Note the null case is when ($p_{mut} = p_{wt} = 0.5$). This is shown with (**A**) low ($\mu = 10^{-9}$) and (**B**) high ($\mu = 10^{-7}$) mutation rate, for individuals with low ($m_0 = 0.001$), medium ($m_0 = 0.01$) and high ($m_0 = 0.1$) initial mutation loads,

and a fixed proportion of transferred mitochondria ($f = 0.5$). Box plots show the median (red line) and distribution (box plot IQR with min/max whiskers and outliers).

Figure 5

Log-likelihood of the models reproducing clinical data of mitochondria mutation load and disease frequency.

Heatmaps showing log-likelihood of reproducing the observed mutation load and disease frequency in humans, for equilibrium conditions under the evolutionary model with (**A**) bottleneck and selection on individuals, (**B**) follicular atresia and selection on cells ($\xi = 5$), (**C**) cytoplasmic transfer with intermediate ($p_{mut} = 0.33$, $p_{wt} = 0.67$, $f = 0.5$) or (**D**) strong ($p_{mut} = 0.25$, $p_{wt} = 0.75$, $f = 0.5$) selective transfer of wildtype mitochondria. Yellow depicts high likelihood; blue, low likelihood. All models are shown for variable bottleneck size (the minimum mitochondria population size at which replication commences) and variable mutation rates.

881

ACKNOWLEDGEMENTS: This work was supported by funding from the Engineering and Physical Sciences Research Council (EP/F500351/1, EP/I017909/1) and Natural Environment Research Council (NE/R010579/1) to AP, the Biotechnology and Biological Sciences Research Council (BB/S003681/1) and bgc3 to NL, and a joint grant to AP and NL from the Biotechnology and Biological Sciences Research Council (BB/V003542/1). We thank Molly Przeworski, David Rand and anonymous reviewer for their perceptive comments on the paper.

DECLARATION OF INTERESTS: none.

DATA AND MATERIALS AVAILABILITY: All code will be posted on Github on publication.

893 **REFERENCES**

894 1. Lynch M, Koskella B, Schaack S. Mutation pressure and the evolution of organelle
895 genomic architecture. Science. 2006;311:1727-39.
896 2. Allio R, Donega S, Galtier N, Nabholz B. Large variation in the ratio of mitochondrial
897 to nuclear mutation rate across animals: Implications for genetic diversity and the use of
898 mitochondrial DNA as a molecular marker. Mol Biol Evol. 2017;34:2762-72.
899 3. Rand DM. The units of selection on mitochondrial DNA. Annu Rev Ecol Sys.
900 2001;32:415-48.
901 4. Elliott HR, Samuels DC, Eden JA, Relton CL, Chinnery PF. Pathogenic mitochondrial
902 DNA mutations are common in the general population. Am J Hum Genet. 2008;83:254-60.
903 5. Schaefer AM, Blakely EL, He L, Whittaker RG, Taylor RW, Chinnery PF, et al.
904 Prevalence of mitochondrial DNA disease in adults. Ann Neurol. 2008;63:35-9.
905 6. Fonseca RR, Johnson WE, Brien SJO, Ramos MJ, Antunes A. The adaptive evolution of
906 the mammalian mitochondrial genome. BMC Genomics. 2008;9:119.
907 7. James JE, Piganeau G, Eyre-Walker A. The rate of adaptive evolution in animal
908 mitochondria. Mol Biol Evol. 2016;25:67-78.
909 8. Yang Z, Nielsen R. Mutation-selection models of codon substitution and their use to
910 estimate selective strengths on codon usage. Mol Biol Evol. 2008;25:568-79.
911 9. Stewart JB, Freyer C, Elson JL, Wredenberg A, Cansu Z, Trufunovic A, et al. Strong
912 purifying selection in transmission of mammalian mitochondrial DNA. PLoS Biol. 2008;6:63-
913 71.
914 10. Fan W, Waymire KG, Narula N, Li P, Rocher C, Coskun PE, et al. A mouse model of
915 mitochondrial disease reveals germline selection against severe mtDNA mutations. Science.
916 2008;319:958-63.
917 11. Hill JH, Chen Z, Xu H. Selective propagation of functional mitochondrial DNA during
918 oogenesis restricts the transmission of a deleterious mitochondrial variant. Nat Genet.
919 2014;46:389-92.
920 12. Burr SP, Pezet M, Chinnery PF. Mitochondrial DNA heteroplasmy and purifying
921 selection in the mammalian female germ line. Dev Growth Differ. 2018;60:21-32.
922 13. Johnston IG, Burgstaller JP, Havlicek V, Kolbe T, Rulicke T, Brem G, et al. Stochastic
923 modelling, bayesian inference, and new in vivo measurements elucidate the debated
924 mtDNA bottleneck mechanism. eLife. 2015;4:e07464.
925 14. Floros VI, Pyle A, Dietmann S, Wei W, Tang WCW, Irie N, et al. Segregation of
926 mitochondrial DNA heteroplasmy through a developmental genetic bottleneck in human
927 embryos. Nat Cell Biol. 2018;20(2):144-51. doi: 10.1038/s41556-017-0017-8.
928 15. Stewart JB, Chinnery PF. The dynamics of mitochondrial DNA heteroplasmy :
929 implications for human health and disease. Nat Rev Genet. 2015;16:530-42.
930 16. Wai T, Teoli D, Shoubridge EA. The mitochondrial DNA genetic bottleneck results
931 from replication of a subpopulation of genomes. Nat Genet. 2008;40:1484-8.
932 17. Cree LM, Samuels DC, de Sousa Lopes SC, Rajasimha HK, Wonnapinij P, Mann JR,
933 Dahl, et al. A reduction of mitochondrial DNA molecules during embryogenesis explains the
934 rapid segregation of genotypes. Nat Genet. 2008;40:249-54.
935 18. Cao L, Shitara H, Sugimoto M, Hayashi J, Abe K, Yonekawa H. New evidence confirms
936 that the mitochondrial bottleneck is generated without reduction of mitochondrial DNA
937 content in early primordial germ cells of mice. PLoS Genet. 2009;5:e1000756.

19. Rebolledo-Jaramillo B, Su MS-W, Stoler N, McElhoe JA, Dickins B, Blankenberg D, et al. Maternal age effect and severe germ-line bottleneck in the inheritance of human mitochondrial DNA. Proc Natl Acad Sci U S A. 2014;111(43):15474. doi: 10.1073/pnas.1409328111.
20. Guo Y, Li C-I, Sheng Q, Winther JF, Cai Q, Boice JD, et al. Very low-level heteroplasmy mtDNA variations are inherited in humans. J Genet Genomics. 2013;40(12):607-15. Epub 2013/12/08. doi: 10.1016/j.jgg.2013.10.003. PubMed PMID: 24377867.
21. Li M, Rothwell R, Vermaat M, Wachsmuth M, Schröder R, Laros JFJ, et al. Transmission of human mtDNA heteroplasmy in the Genome of the Netherlands families: support for a variable-size bottleneck. Genome Res. 2016;26(4):417-26. Epub 2016/02/25. doi: 10.1101/gr.203216.115. PubMed PMID: 26916109.
22. Bergstrom C, Pritchard J. Germline bottlenecks and the evolutionary maintenance of mitochondrial genomes. Genetics. 1998;149(4):2135-46. PubMed PMID: 9691064.
23. Roze D, Rousset F, Michalakis Y. Germline bottlenecks, biparental inheritance and selection on mitochondrial variants: a two-level selection model. Genetics. 2005;170(3):1385-99. Epub 2005/05/23. doi: 10.1534/genetics.104.039495. PubMed PMID: 15911581.
24. Hadjivasiliou Z, Lane N, Seymour RM, Pomiankowski A. Dynamics of mitochondrial inheritance in the evolution of binary mating types and two sexes. Proc R Soc B Biol Sci. 2013;280:20131920.
25. Radzvilavicius AL, Lane N, Pomiankowski A. Sexual conflict explains the extraordinary diversity of mechanisms regulating mitochondrial inheritance. BMC Biol. 2017;14.
26. Krakauer DC, Mira A. Mitochondria and germ-cell death. Nature. 1999;400:125-6.
27. Chu H. P., Liao Y, Novak JS, Hu Z, Merkin JJ, Shymkiv Y, et al. Germline quality control : eEF2K stands guard to eliminate defective oocytes. Dev Cell. 2014;28:561-72.
28. Haig D. Intracellular evolution of mitochondrial DNA (mtDNA) and the tragedy of the cytoplasmic commons. BioEssays. 2016;38:549-55.
29. Albamonte MS WM, Albamonte MI, Jensen F, Espinosa MB, and Vitullo AD. The developing human ovary : immunohistochemical analysis of germ-cell-specific VASA protein, BCL-2 / BAX expression balance and apoptosis. Hum Reprod. 2008;23:1895-901.
30. Kaipia A, Hsueh AJW. Regulation of ovarian follicle atresia. Annual Review of Physiology. 1997;59(1):349-63. doi: 10.1146/annurev.physiol.59.1.349.
31. Townson DH, Combelles CMH. Ovarian Follicular Atresia. Darwish A, editor: InTech; 2012.
32. Suganuma N, Kitagawa T, Nawa A, Tomoda Y. Human ovarian aging and mitochondrial DNA deletion. Horm Res. 1993;39:16-21. Epub 1993/01/01. doi: 10.1159/000182752. PubMed PMID: 8365704.
33. Galimov ER, Chernyak BV, Sidorenko AS, Tereshkova AV, Chumakov PM. Prooxidant properties of p66shc are mediated by mitochondria in human cells. PLoS One. 2014;9(3):e86521-e. doi: 10.1371/journal.pone.0086521. PubMed PMID: 24618848.
34. Cummins JM. The role of mitochondria in the establishment of oocyte functional competence. Eur J Obstet Gynecol Reprod Biol. 2004;115:S23-9. doi: https://doi.org/10.1016/j.ejogrb.2004.01.011.
35. Nezis IP, Stravopodis DJ, Papassideri I, Robert-Nicoud M, Margaritis LH. Stage-specific apoptotic patterns during Drosophila oogenesis. European Journal of Cell Biology. 2000;79(9):610-20. doi: https://doi.org/10.1078/0171-9335-00088.

984 36. Rodrigues P, Limback D, McGinnis LK, Plancha CE, Albertini DF. Multiple mechanisms
985 of germ cell loss in the perinatal mouse ovary. Reproduction. 2009;137(4):709-20.
986 37. Saidapur SK. Follicular atresia in the ovaries of nonmammalian vertebrates.
987 International review of cytology. 1978;54:225-44.
988 38. Morita Y, Tilly JL. Oocyte apoptosis: like sand through an hourglass. Developmental
989 biology. 1999;213(1):1-17.
990 39. Tilly JL. Commuting the death sentence: how oocytes strive to survive. Nat Rev Mol
991 Cell Biol. 2001;2:838-48.
992 40. Perez GI, Trbovich AM, Gosden RG, Tilly JL. Mitochondria and the death of oocytes.
993 Nature. 2000;403(6769):500-1. doi: 10.1038/35000651.
994 41. Lei L, Spradling AC. Mouse oocytes differentiate through organelle enrichment from
995 sister cyst germ cells. Science. 2016;252:95-9.
996 42. Motta PM, Nottola SA, Makabe S, Heyn R. Mitochondrial morphology in human fetal
997 and adult female germ cells. Human Reproduction. 2000;15(suppl_2):129-47. doi:
998 10.1093/humrep/15.suppl_2.129.
999 43. Hertig AT. The primary human oocyte: some observations on the fine structure of
1000 Balbiani's vitelline body and the origin of the annulate lamellae. American Journal of
1001 Anatomy. 1968;122(1):107-37.
1002 44. Kloc M, Bilinski S, Etkin LD. The Balbiani body and germ cell determinants: 150 years
1003 later. Curr Top Dev Biol. 2004;59:1-36.
1004 45. Tworzydlo W, Kisiel E, Jankowska W, Witwicka A, Bilinski SM. Exclusion of
1005 dysfunctional mitochondria from Balbiani body during early oogenesis of Thermobia. Cell
1006 Tissue Res. 2016;366(1):191-201. Epub 2016/05/10. doi: 10.1007/s00441-016-2414-x.
1007 PubMed PMID: 27164893.
1008 46. Reunov A, Alexandrova Y, Reunova Y, Komkova A, Milani L. Germ plasm provides
1009 clues on meiosis: the concerted action of germ plasm granules and mitochondria in
1010 gametogenesis of the clam Ruditapes philippinarum. Zygote. 2019;27(1):25-35. Epub
1011 2018/12/07. doi: 10.1017/S0967199418000588.
1012 47. Larkman AU. The fine structure of mitochondria and the mitochondrial cloud during
1013 oogenesis on the sea anemone Actinia. Tissue and Cell. 1984;16:393-404.
1014 48. Heasman J, Quarmby J, Wylie CC. The mitochondrial cloud of Xenopus oocytes: The
1015 source of germinal granule material. Developmental Biology. 1984;105(2):458-69. doi:
1016 https://doi.org/10.1016/0012-1606(84)90303-8.
1017 49. Pepling ME, Wilhelm JE, Hara AL, Gephardt GW, Spradling AC. Mouse oocytes within
1018 germ cell cysts and primordial follicles contain a Balbiani body. Proc Natl Acad Sci U S A.
1019 2007;104(1):187. doi: 10.1073/pnas.0609923104.
1020 50. Zhou RR, Wang B, Wang J, Schatten H, Zhang YZ. Is the mitochondrial cloud the
1021 selection machinery for preferentially transmitting wild-type mtDNA between generations?
1022 Rewinding Müller's ratchet efficiently. Curr Genet. 2010;56:101-7.
1023 51. Bilinski SM, Kloc M, Tworzydlo W. Selection of mitochondria in female germline cells:
1024 is Balbiani body implicated in this process? J Assist Reprod Genet. 2017;34:1405-12.
1025 52. Moore AS, Coscia SM, Simpson CL, Ortega FE, Wait EC, Heddleston JM, et al. Actin
1026 cables and comet tails organize mitochondrial networks in mitosis. Nature.
1027 2021;591(7851):659-64. doi: 10.1038/s41586-021-03309-5.
1028 53. Taguchi N, Ishihara N, Jofuku A, Oka T, Mihara K. Mitotic phosphorylation of
1029 dynamin-related GTPase Drp1 participates in mitochondrial fission. J Biol Chem.

2007;282(15):11521-9. Epub 2007/02/16. doi: 10.1074/jbc.M607279200. PubMed PMID: 17301055.
54. Park YY, Cho H. Mitofusin 1 is degraded at G2/M phase through ubiquitylation by MARCH5. Cell Div. 2012;7(1):25. Epub 2012/12/21. doi: 10.1186/1747-1028-7-25. PubMed PMID: 23253261; PubMed Central PMCID: PMCPMC3542011.
55. Dumollard R, Duchen M, Carroll J. The role of mitochondrial function in the oocyte and embryo. Curr Top Dev Biol. 2007;77:21-49.
56. Extavour CG, Akam M. Mechanisms of germ cell specification across the metazoans: epigenesis and preformation. Development. 2003;130:5869-84.
57. Stewart JB, Larsson N-G. Keeping mtDNA in shape between generations. PLoS Genet. 2014;10(10):e1004670-e. doi: 10.1371/journal.pgen.1004670. PubMed PMID: 25299061.
58. Allen J, de Paula W. Mitochondrial genome function and maternal inheritance. Biochem Soc Trans. 2013;41:1298-304.
59. Radzvilavicius AL, Hadjivasiliou Z, Pomiankowski A, Lane N. Selection for mitochondrial quality drives evolution of the germline. PLoS Biol. 2016;14:e2000410.
60. Rossignol R, Faustin B, Rocher C, Malgat M, Mazat JP, Letellier T. Mitochondrial threshold effects. Biochem J. 2003;370:751-62.
61. Kopinski PK, Janssen KA, Schaefer PM, Trefely S, Perry CE, Potluri P, et al. Regulation of nuclear epigenome by mitochondrial DNA heteroplasmy. Proc Natl Acad Sci U S A. 2019;116(32):16028-35. Epub 2019/06/30. doi: 10.1073/pnas.1906896116. PubMed PMID: 31253706; PubMed Central PMCID: PMCPMC6689928.
62. Wallace DC, Chalkia D. Mitochondrial DNA genetics and the heteroplasmy conundrum in evolution and disease. Cold Spring Harb Perspect Biol. 2013;5:a021220.
63. Chen Z, Wang ZH, Zhang G, Bleck CKE, Chung DJ, Madison GP, et al. Mitochondrial DNA segregation and replication restrict the transmission of detrimental mutation. J Cell Biol. 2020;219(7). Epub 2020/05/07. doi: 10.1083/jcb.201905160. PubMed PMID: 32375181; PubMed Central PMCID: PMCPMC7337505.
64. Pepling ME. From primordial germ cell to primordial follicle: mammalian female germ cell development. Genesis. 2006;44(12):622-32. doi: 10.1002/dvg.20258.
65. de Paula WBM, Lucas CH, Agip A-NA, Vizcay-Barrena G, Allen JF. Energy, ageing, fidelity and sex: oocyte mitochondrial DNA as a protected genetic template. Philos Trans R Soc B. 2013;368(1622):20120263. doi: 10.1098/rstb.2012.0263.
66. Arbeithuber B, Hester J, Cremona MA, Stoler N, Zaidi A, Higgins B, et al. Age-related accumulation of de novo mitochondrial mutations in mammalian oocytes and somatic tissues. PLOS Biol. 2020;18(7):e3000745. doi: 10.1371/journal.pbio.3000745.
67. Trifunovic A, Hansson A, Wredenberg A, Rovio AT, Dufour E, Khvorostov I, et al. Somatic mtDNA mutations cause aging phenotypes without affecting reactive oxygen species production. Proc Natl Acad Sci U S A. 2005;102(50):17993-8. Epub 2005/12/08. doi: 10.1073/pnas.0508886102. PubMed PMID: 16332961; PubMed Central PMCID: PMCPMC1312403.
68. Lanfear L. Do plants have a segregated germline? PLoS Biol. 2018;16:e2005439.
69. Extavour CG. Evolution of the bilaterian germ line: lineage origin and modulation of specification mechanisms. Integrative and comparative biology. 2007;47(5):770-85.
70. Blackstone NW, Jasker BD. Phylogenetic considerations of clonality, coloniality, and mode of germline development in animals. Journal of Experimental Zoology Part B: Molecular and Developmental Evolution. 2003;297(1):35-47.

71. Cox RT, Spradling AC. A Balbiani body and the fusome mediate mitochondrial inheritance during *Drosophila* oogenesis. Development. 2003;130(8):1579. doi: 10.1242/dev.00365.
72. Twig G, Elorza A, Molina AJA, Mohamed H, Wikstrom JD, Walzer G, et al. Fission and selective fusion govern mitochondrial segregation and elimination by autophagy. EMBO J. 2008;27(2):433-46. doi: 10.1038/sj.emboj.7601963.
73. Kim I, Rodriguez-Enriquez S, Lemasters JJ. Selective degradation of mitochondria by mitophagy. Arch Biochem Biophys. 2007;462(2):245-53. doi: https://doi.org/10.1016/j.abb.2007.03.034.
74. Dalton CM, Carroll J. Biased inheritance of mitochondria during asymmetric cell division in the mouse oocyte. J Cell Sci. 2013;126(13):2955-64. Epub 2013/05/09. doi: 10.1242/jcs.128744. PubMed PMID: 23659999.
75. Sigurdardottir S, Helgason A, Gulcher JR, Donnelly P. The mutation rate in the human mtDNA control region. Am J Hum Genet. 2000;66:1599-609.
76. Stewart JB, Chinnery PF. The dynamics of mitochondrial DNA heteroplasmy: implications for human health and disease. Nat Rev Genet. 2015;16(9):530-42. Epub 2015/08/19. doi: 10.1038/nrg3966. PubMed PMID: 26281784.
77. Shoubridge EA, Wai T. Mitochondrial DNA and the mammalian oocyte. Curr Top Dev Biol. 2007;77:87-111. Epub 2007/01/16. doi: 10.1016/s0070-2153(06)77004-1. PubMed PMID: 17222701.
78. Lane N. Power, Sex, Suicide: Mitochondria and the Meaning of Life: Oxford University Press; 2005.
79. Pereira CV, Gitschlag BL, Patel MR. Cellular mechanisms of mtDNA heteroplasmy dynamics. Critical Reviews in Biochemistry and Molecular Biology. 2021:1-16.
80. Carelli V, Maresca A, Caporali L, Trifunov S, Zanna C, Rugolo M. Mitochondria: biogenesis and mitophagy balance in segregation and clonal expansion of mitochondrial DNA mutations. The international journal of biochemistry & cell biology. 2015;63:21-4.
81. Diot A, Morten K, Poulton J. Mitophagy plays a central role in mitochondrial ageing. Mammalian Genome. 2016;27(7):381-95.
82. Buss L. The Evolution of Individuality: Princeton University Press; 1987.
83. Maynard Smith J, Szathmáry E. The Major Transitions in Evolution: Oxford University Press; 1995.
84. Reynier P, May-Panloup P, Chretien M, Morgan C, Jean M, Savagner F, et al. Mitochondrial DNA content affects the fertilizability of human oocytes. Molecular human reproduction. 2001;7(5):425-9.
85. Palca J. The other human genome. Science. 1990;249:1104-5.
86. Kullback S, Leibler RA. On Information and Sufficiency. Ann Math Statist. 1951;22(1):79-86. doi: 10.1214/aoms/1177729694.
87. Xu S, Schaack S, Seyfert A, Choi E, Lynch M, Cristescu ME. High mutation rates in the mitochondrial genomes of *Daphnia pulex*. Mol Biol Evol. 2012;29(2):763-9. Epub 2011/10/13. doi: 10.1093/molbev/msr243. PubMed PMID: 21998274.
88. Denver DR, Morris K, Lynch M, Vassilieva LL, Thomas WK. High Direct Estimate of the Mutation Rate in the Mitochondrial Genome of *Caenorhabditis elegans*. Science. 2000;289(5488):2342. doi: 10.1126/science.289.5488.2342.
89. Haag-Liautard C, Coffey N, Houle D, Lynch M, Charlesworth B, Keightley PD. Direct estimation of the mitochondrial DNA mutation rate in *Drosophila melanogaster*. PLoS Biol. 2008;6(8):e204. doi: 10.1371/journal.pbio.0060204. PubMed PMID: 18715119.

1123

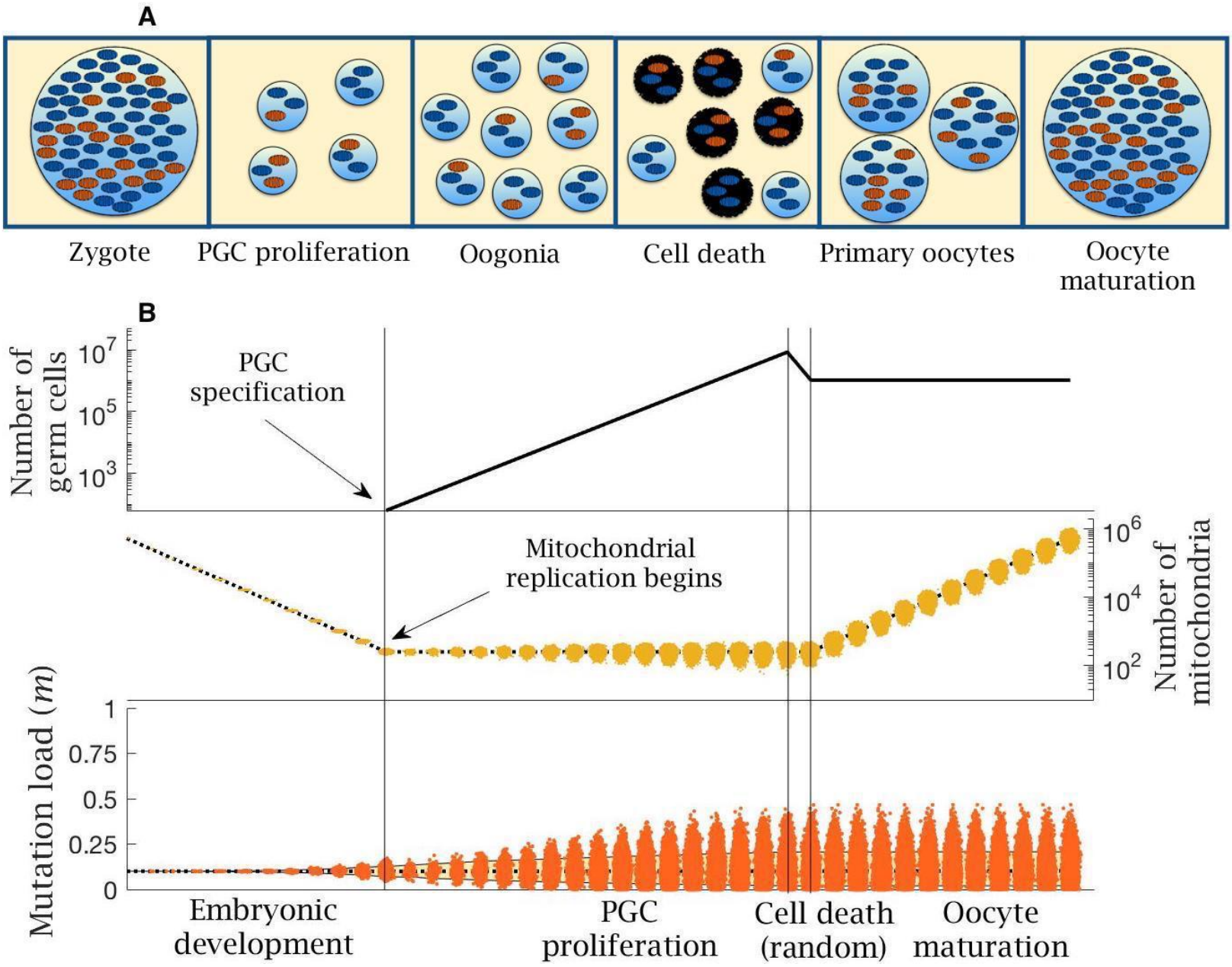
A
Zygote
PGC proliferation
Oogonia
Cell death
Primary oocytes
Oocyte maturation
B
Number of germ cells
10^7
10^5
10^3
PGC specification
Mitochondrial replication begins
10^6
10^4
10^2
Number of mitochondria
Mutation load (m)
1
0.75
0.5
0.25
0
Embryonic development
PGC proliferation
Cell death (random)
Oocyte maturation

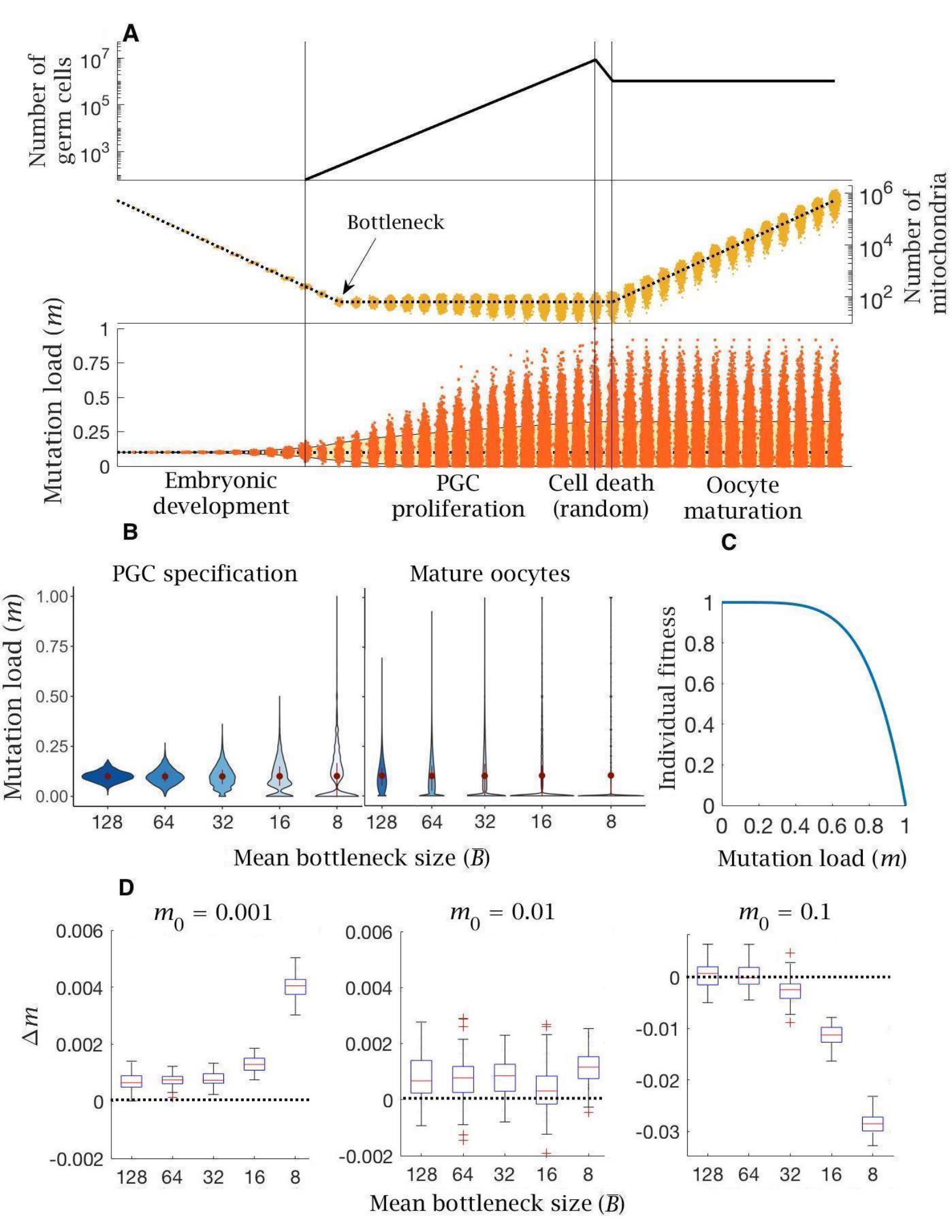
A
Number of germ cells
10^7
10^5
10^3
Bottleneck
10^6
10^4
10^2
Number of mitochondria
Mutation load (m)
1
0.75
0.5
0.25
0
Embryonic development
PGC proliferation
Cell death (random)
Oocyte maturation
B
PGC specification
Mature oocytes
Mutation load (m)
1.00
0.75
0.50
0.25
0.00
128 64 32 16 8 128 64 32 16 8
Mean bottleneck size ($\bar{B}$)
C
Individual fitness
1
0.8
0.6
0.4
0.2
0
0 0.2 0.4 0.6 0.8 1
Mutation load (m)
D
$m_0 = 0.001$
$m_0 = 0.01$
$m_0 = 0.1$
Δm
0.006
0.004
0.002
0
-0.002
-0.01
-0.02
-0.03
128 64 32 16 8
Mean bottleneck size ($\bar{B}$)

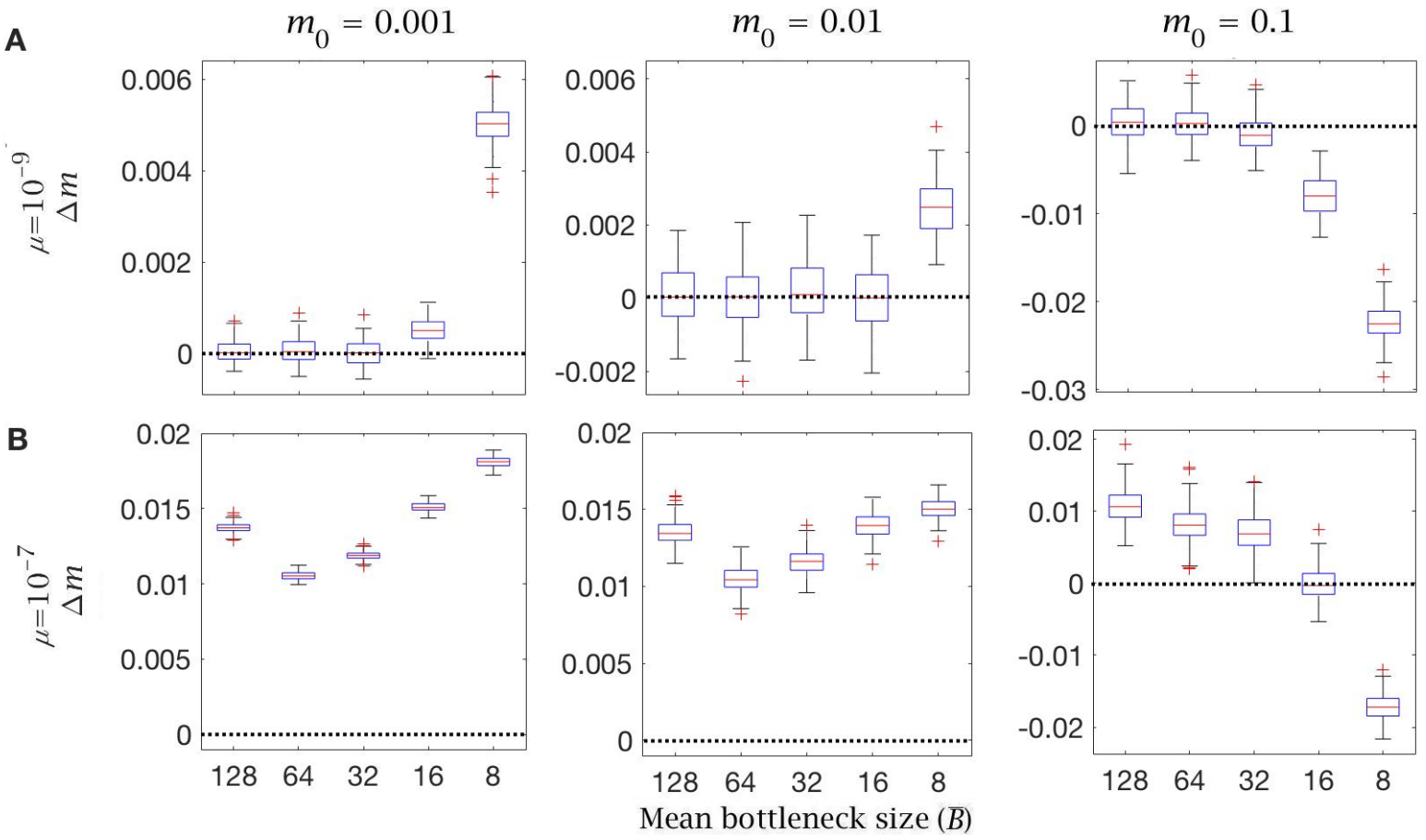
A
B
$m_0 = 0.001$
$m_0 = 0.01$
$m_0 = 0.1$
$\mu=10^{-9}$ Δm
$\mu=10^{-7}$ Δm
0.006
0.004
0.002
0
-0.002
0.02
0.015
0.01
0.005
-0.01
-0.02
-0.03
128 64 32 16 8
Mean bottleneck size ($\bar{B}$)

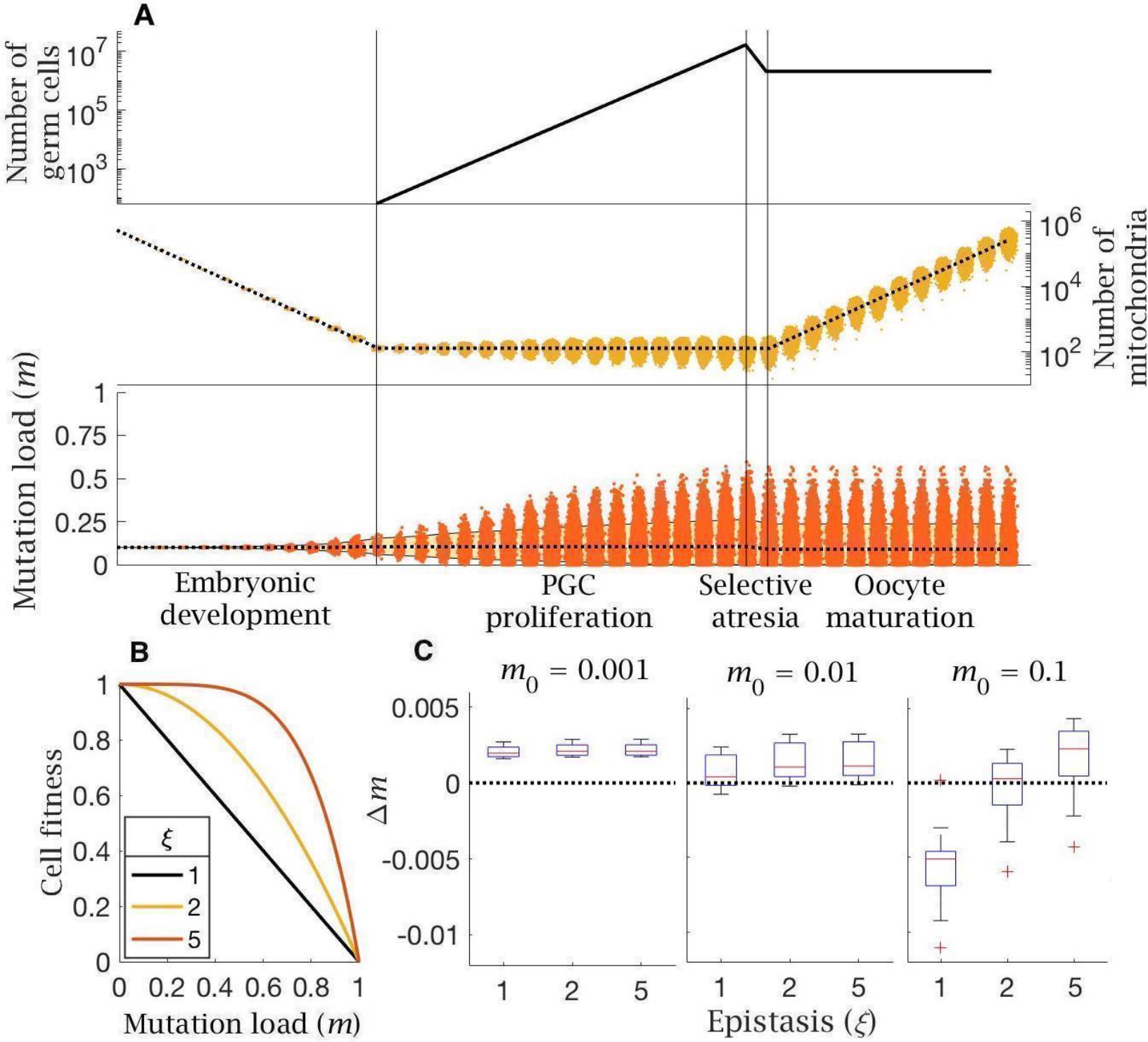
A
Number of germ cells
10^7
10^5
10^3
10^6
10^4
10^2
Number of mitochondria
Mutation load (m)
1
0.75
0.5
0.25
0
Embryonic development
PGC proliferation
Selective atresia
Oocyte maturation
B
Cell fitness
1
0.8
0.6
0.4
0.2
0
ξ
1
2
5
0 0.2 0.4 0.6 0.8 1
Mutation load (m)
C
$m_0 = 0.001$
$m_0 = 0.01$
$m_0 = 0.1$
Δm
0.005
0
-0.005
-0.01
1 2 5
Epistasis (ξ)

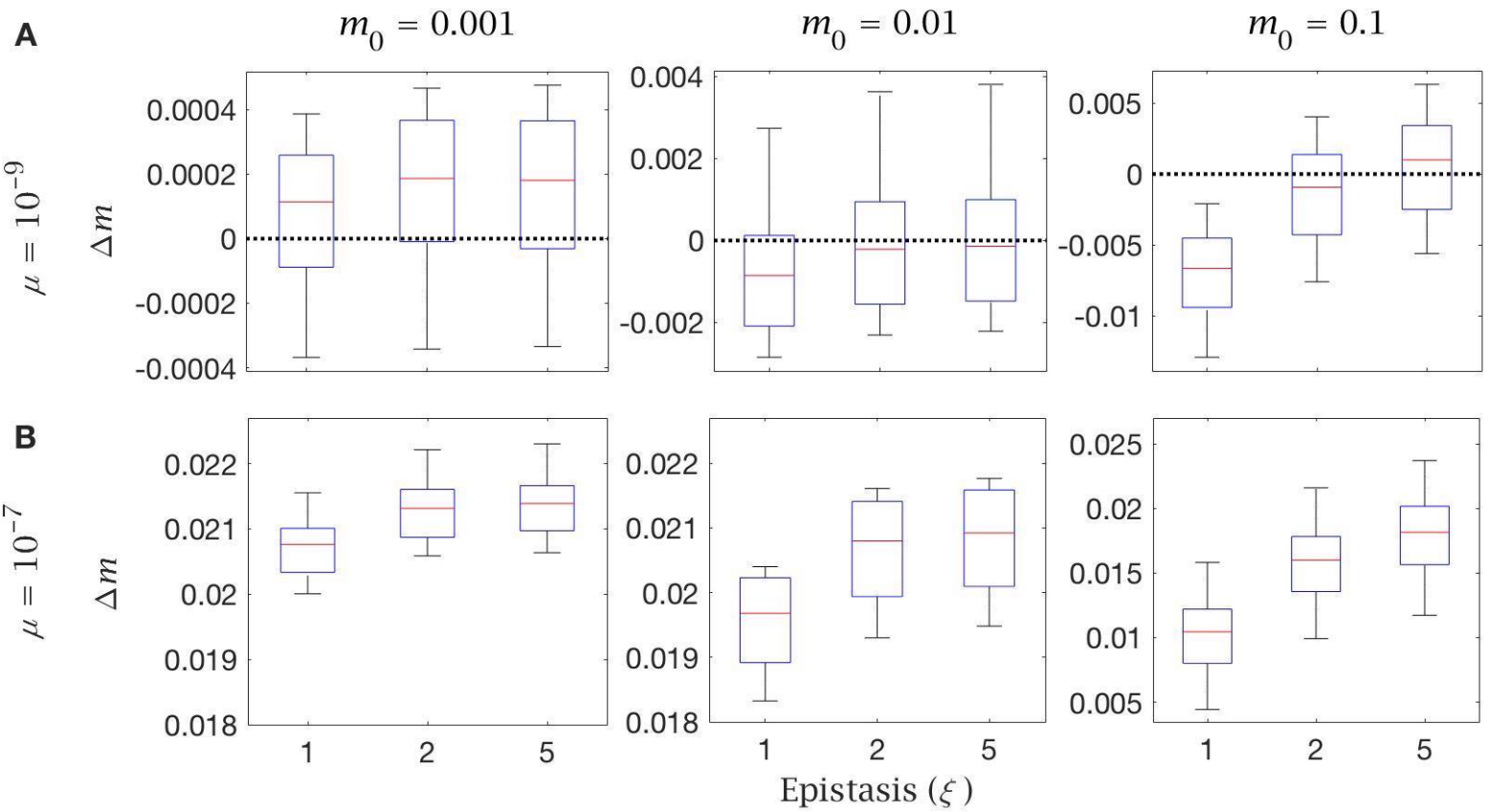
A
B
$m_0 = 0.001$
$m_0 = 0.01$
$m_0 = 0.1$
$\mu = 10^{-9}$
$\mu = 10^{-7}$
Δm
0.0004
0.0002
0
-0.0002
-0.0004
0.004
0.002
0
-0.002
0.005
0
-0.005
-0.01
0.022
0.021
0.02
0.019
0.018
0.025
0.02
0.015
0.01
0.005
1
2
5
Epistasis (ξ)

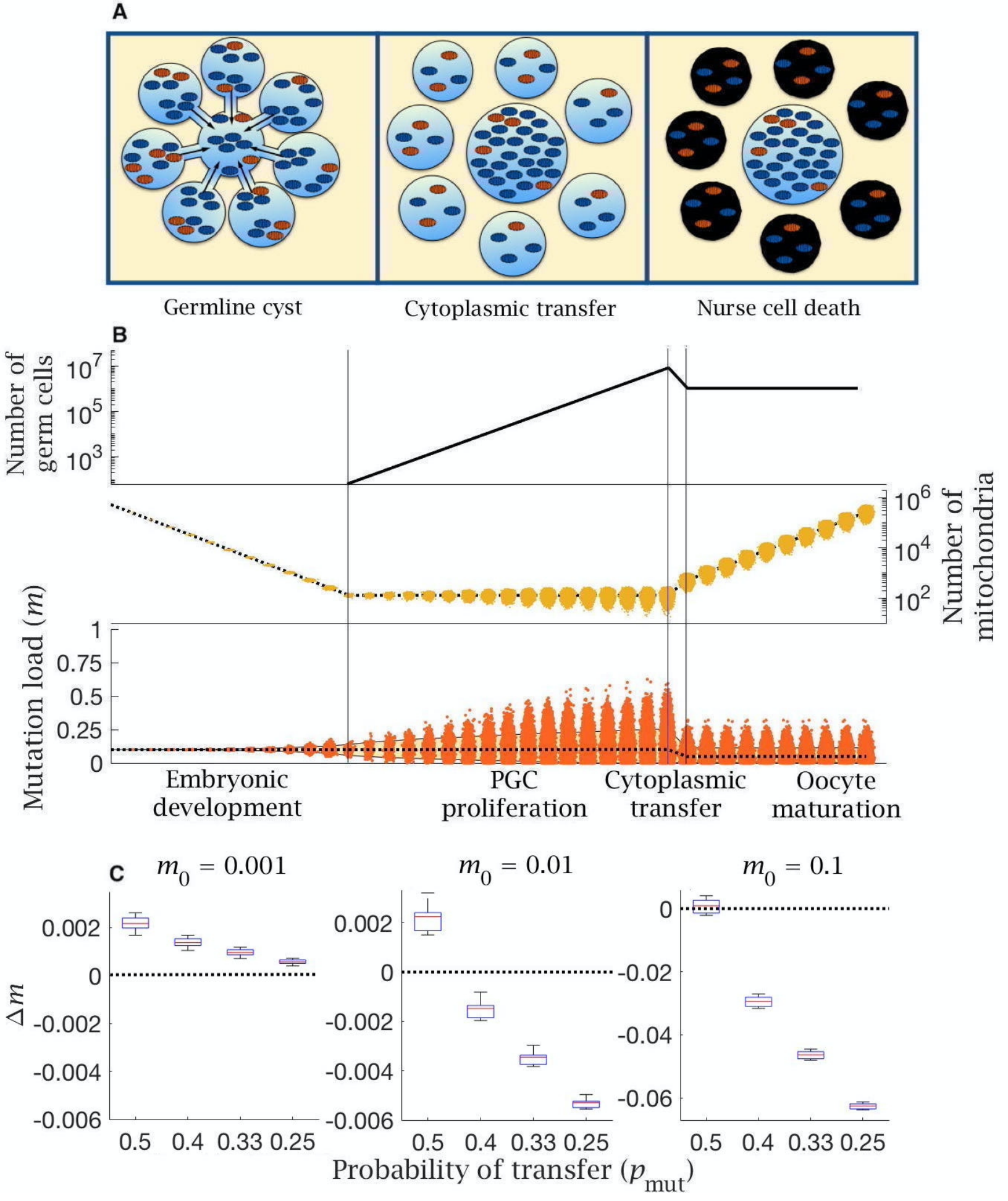
A
Germline cyst
Cytoplasmic transfer
Nurse cell death
B
Number of germ cells
10^7
10^5
10^3
10^6
10^4
10^2
Number of mitochondria
Mutation load (m)
1
0.75
0.5
0.25
0
Embryonic development
PGC proliferation
Cytoplasmic transfer
Oocyte maturation
C
$m_0 = 0.001$
$m_0 = 0.01$
$m_0 = 0.1$
Δm
0.002
0
-0.002
-0.004
-0.006
-0.02
-0.04
-0.06
0.5 0.4 0.33 0.25
Probability of transfer (p_{mut})

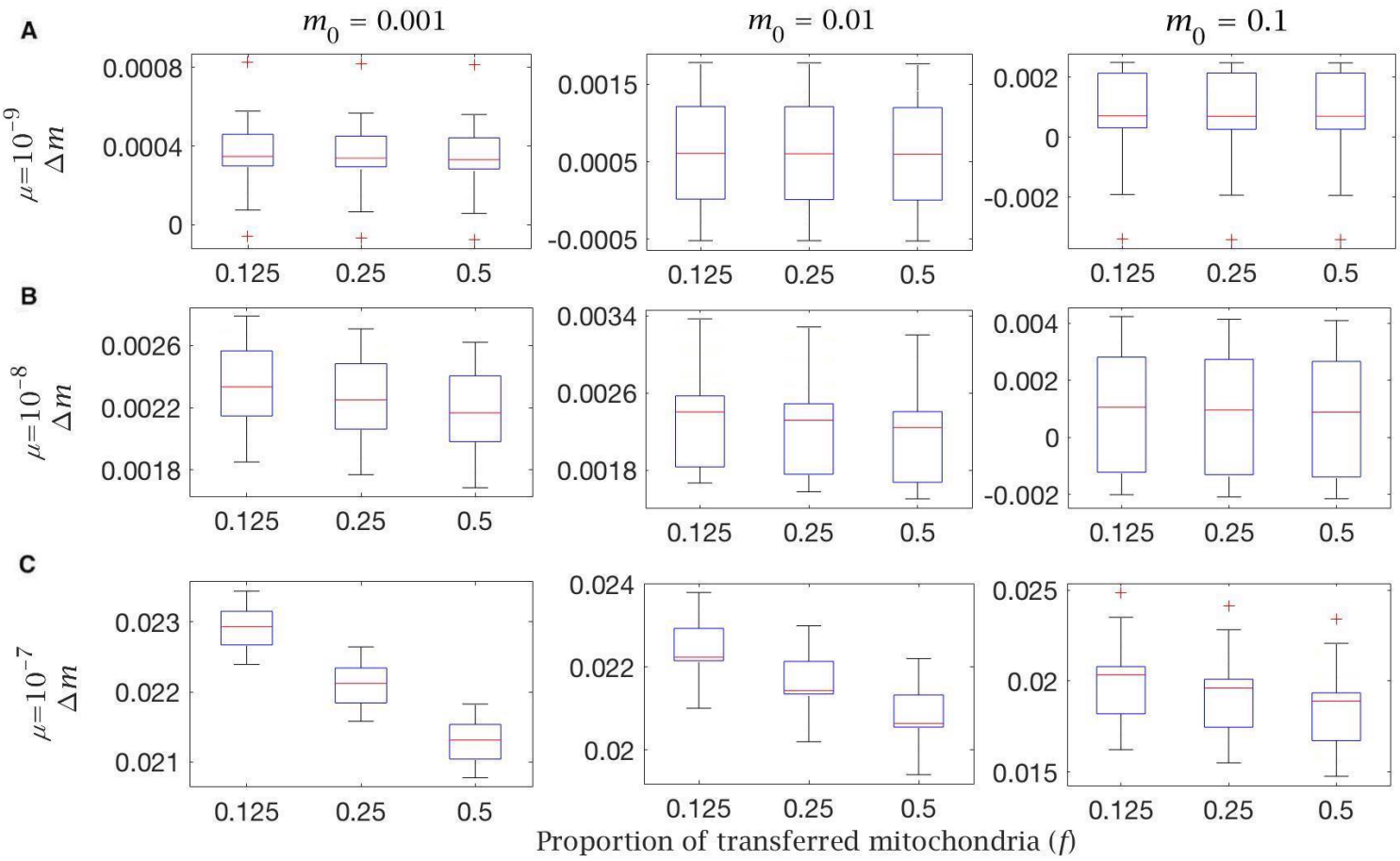
A
B
C
m_0 = 0.001
m_0 = 0.01
m_0 = 0.1
μ=10^{-9} Δm
μ=10^{-8} Δm
μ=10^{-7} Δm
0.0008
0.0004
0
0.0015
0.0005
-0.0005
0.002
0
-0.002
0.0026
0.0022
0.0018
0.0034
0.0026
0.0018
0.004
0.002
0
-0.002
0.023
0.022
0.021
0.024
0.022
0.02
0.025
0.02
0.015
0.125
0.25
0.5
Proportion of transferred mitochondria (f)

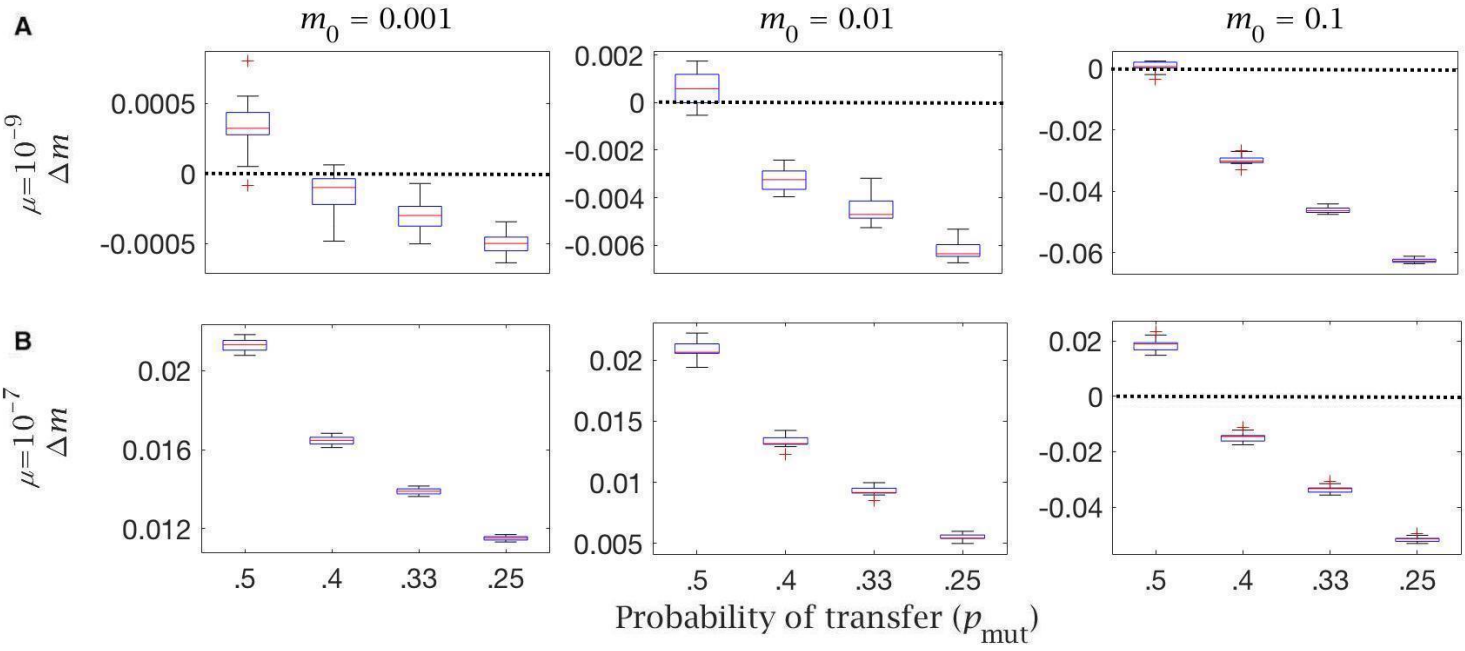
A
m_0 = 0.001
m_0 = 0.01
m_0 = 0.1
μ=10^{-9} Δm
0.0005
0
-0.0005
0.002
0
-0.002
-0.004
-0.006
0
-0.02
-0.04
-0.06
B
μ=10^{-7} Δm
0.02
0.016
0.012
0.02
0.015
0.01
0.005
0.02
0
-0.02
-0.04
.5
.4
.33
.25
Probability of transfer (p_{mut})

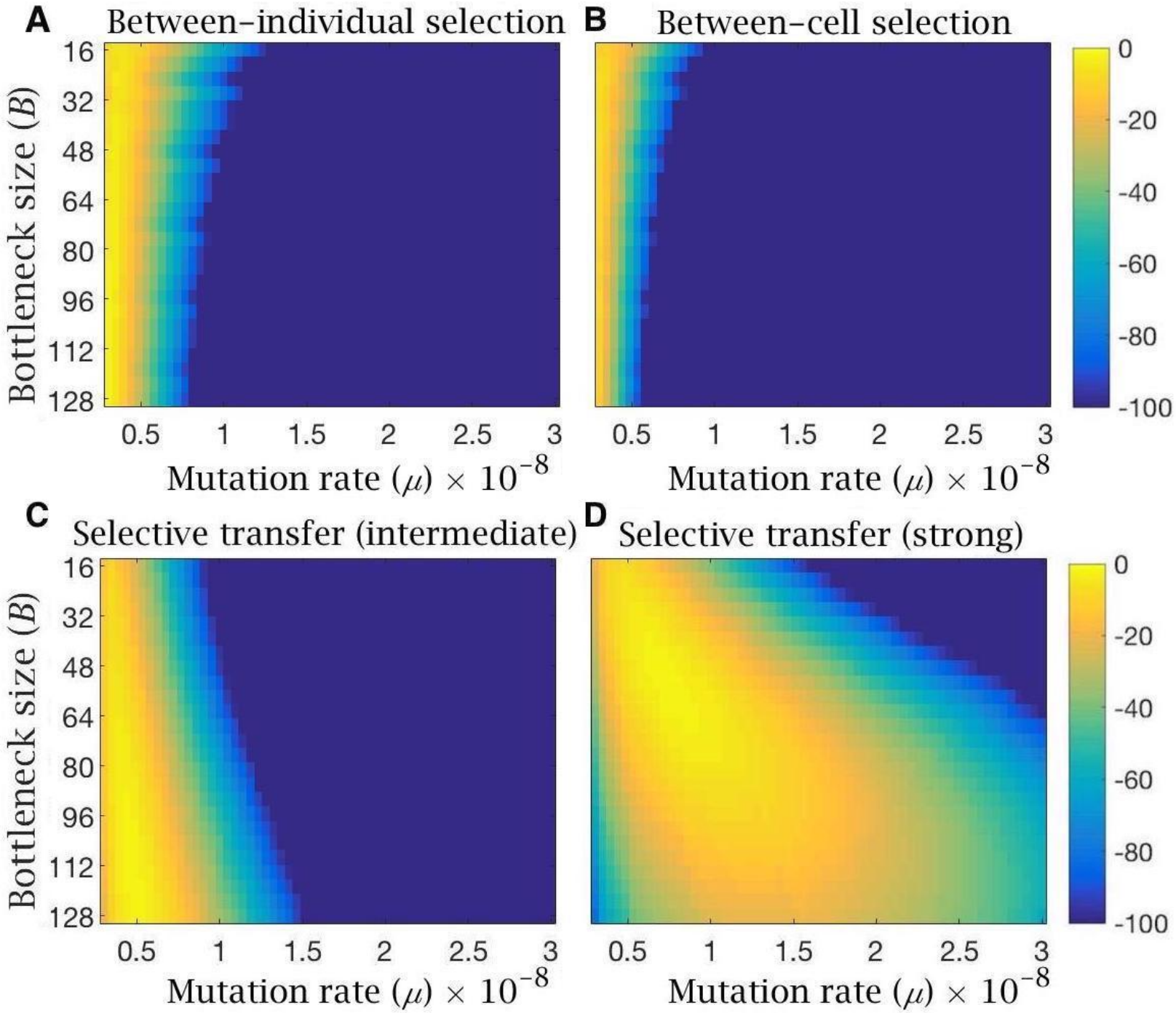
A
Between–individual selection
B
Between–cell selection
C
Selective transfer (intermediate)
D
Selective transfer (strong)
Bottleneck size (B)
16
32
48
64
80
96
112
128
0.5
1
1.5
2
2.5
3
Mutation rate (μ) $\times$ 10^{-8}
0
-20
-40
-60
-80
-100